NRC Research and/or Technical Assistance Rept

PDR

EGG-NTAP-6032

September 1982

BEST ESTIMATE ANALYSIS OF A SMALL BREAK LOCA IN A RESAR-3S PRESSURIZED WATER REACTOR

J. E. Blakeley
J. M. Cozzuol

Idaho National Engineering Laboratory
Operated by the U.S. Department of Energy

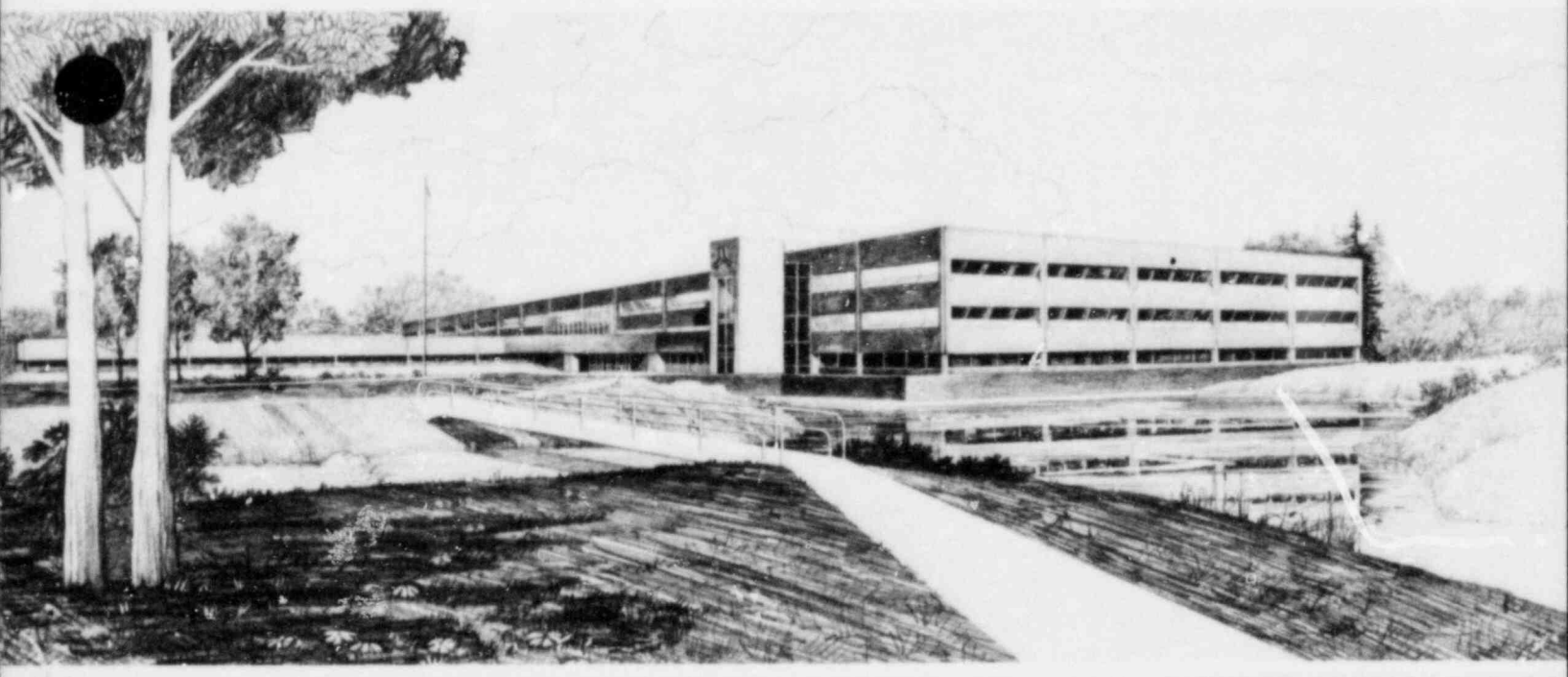

This is an informal report intended for use as a preliminary or working document

Prepared for the
U.S. NUCLEAR REGULATORY COMMISSION
Under DOE Contract No. DE-AC07-76ID01570
FIN No. A6468

EG&G Idaho

EG&G Idaho, Inc.

FORM EG&G-398
Rev. 03-82

INTERIM REPORT

Accession No. _____

Report No. EGG-NTAP-6032

Contract Program or Project Title: NRC Technical Assistance Program Division

Subject of this Document: BEST ESTIMATE ANALYSIS OF A SMALL BREAK LOCA IN A RESAR-3S PRESSURIZED WATER REACTOR

Type of Document: Technical Report

Author(s): J. E. Blakeley, J. M. Cozzuol

Date of Document: September 1982

Responsible NRC Individual and NRC Office or Division: Jack Guttman, NRC-DSI

This document was prepared primarily for preliminary or internal use. It has not received full review and approval. Since there may be substantive changes, this document should not be considered final.

EG&G Idaho, Inc.
Idaho Falls, Idaho **83415**

Prepared for the
U.S. Nuclear Regulatory Commission
Washington, D.C.
Under DOE Contract No. **DE-AC07-76ID01570**
NRC FIN No. A6468

INTERIM REPORT

ABSTRACT

The RELAP5/MOD1 computer code was used to calculate the system response of a Westinghouse RESAR-3S plant to a limiting small cold leg break. Best estimate assumptions were used in the calculation for the purpose of verifying and quantifying the conservatisms inherent within the analytical methodology required by 10 CFR 50.46 and Appendix K to 10 CFR 50. Results of the analysis of the best estimate small break calculation indicate a continuous primary system depressurization with only brief periods of dryout of the top third of the core, and with peak cladding temperatures remaining less than steady state full power cladding temperatures. Comparisons of the RELAP5 results with results obtained from a Westinghouse evaluation model calculation for the limiting small break in a RESAR-3S plant show that the requirements for evaluation model small break calculations specified by 10 CFR 50.46 and Appendix K to 10 CFR 50 result in significant conservatisms in calculated system response relative to best estimate calculations.

FIN No. A6468--RESAR-3S "Most Probable" Best-Estimate LOCA Analyses in Support of FSAR Reviews

SUMMARY

The RELAP5/MOD1 systems thermal-hydraulic code was used to calculate the response of a Westinghouse RESAR-3S pressurized water reactor (PWR) to a small cold leg break. The Westinghouse RESAR-3S system is a large, 3411 MW thermal, 4-loop PWR. The system was modeled with the RELAP5 computer program with three intact loops combined into a single loop, and with the fourth loop containing a break which represented a 0.08727 ft^2 crack in the primary system piping where the accumulator line connects with the cold leg piping. The chosen break size is the limiting small break size, as documented in the Westinghouse RESAR-3S Final Safety Analysis Report. Best estimate assumptions were used in the RELAP5 calculation for the purpose of providing a basis for verifying and quantifying the conservatisms inherent in the Westinghouse evaluation model (EM) RESAR-3S calculations as required by 10 CFR 50.46 and Appendix K to 10 CFR 50.

Analysis of the results of the RELAP5 calculation indicate that the system response to the small cold leg break is characterized by a continuous primary side depressurization, with only brief periods of dryout of the top third of the core. The periods of dryout occur just prior to blowout of the loop seal, and again after initiation of accumulator injection. However, fuel rod cladding temperature increases are limited, and peak cladding temperatures during periods of dryout are substantially less than the steady state full power cladding temperature.

The comparisons of results from the RELAP5 best estimate calculation with the results from the Westinghouse evaluation model calculation illustrates the conservatisms inherent in the evaluation model analytical methodology. In particular, the EM calculation shows a relatively prolonged period when the upper half of the core is uncovered, and during which cladding temperatures increased to a maximum of about 1760°F. This compares to the best estimate calculation which shows only brief periods when the top of the core is uncovered and maximum fuel rod cladding temperature increases during these periods of only about 30°F.

FOREWORD

The RESAR-3S "Most Probable" Best Estimate LOCA Analyses in support of FSAR Reviews project was conducted under the direction of NRC's Division of Systems Integration, Roger Mattson, Director; Themis Speis, Assistant Director for Reactor Safety; Brian Sheron, Branch Chief for Reactor Systems; Norm Lauben, RSB Section Leader; and Jack Guttmann, Project Manager/Technical Monitor. EG&G Idaho personnel involved in the project were Tom Charlton, Branch Manager, Reactor Simulation and Analysis Branch; Dr. Andy Peterson, Supervisor, PWR Systems Analysis; Tom Laats, Supervisor, Fuels Analysis and Data Bank; James Cozzuol, Jeb Blakeley, and Don Fletcher, Engineers; Joan Mosher, Glada Gatenby, and Brenda Hendrickson, Word Processing; Erma Jenkins and Sindi Crowton, Data Technicians. This project was completed in September 1982 under FIN Number A6468 and NRC B&R Number 20 19 40 42 3.

CONTENTS

FIGURES

TABLES

BEST ESTIMATE ANALYSIS OF A SMALL BREAK LOCA IN A RESAR-3S PRESSURIZED WATER REACTOR

1. INTRODUCTION

Current requirements for determining the acceptability of emergency core cooling (ECC) systems in light water reactors during postulated loss-of-coolant accidents (LOCA) incorporate conservatisms developed to bound the uncertainties in the analysis of the phenomena that occur. These conservatisms are codified in 10 CFR 50.46 and Appendix K to 10 CFR 50. Calculations have been performed with sophisticated analytical computer programs as part of an effort to verify and quantify the conservatisms inherent in the requirements of 10 CFR 50.

This report documents the results of a postulated 4 inch cold leg break LOCA analysis of a Westinghouse pressurized water reactor (PWR) assuming most probable operating parameters and utilizing the best available analytical methodology. The PWR design selected was the Westinghouse RESAR-3S nuclear steam supply system (NSSS). Drawings and plant data supplied by Westinghouse were used to construct a computer model representing the system geometry and operating conditions. The computer code selected for the analysis was the RELAP5/MOD1 computer code[1] developed at the Idaho National Engineering Laboratory for small break LOCAs.

Section 2 of this report contains a description of the plant and the small break LOCA calculation that was performed. Details of the RELAP5/MOD1 nodalization used to represent the RESAR-3S system are given in Section 3 along with the code options selected for the calculation. Section 4 highlights the differences in the assumptions used for the RELAP5 most probable best estimate calculation and those used in the Westinghouse evaluation model (EM) calculation. Section 5 compares the boundary and initial conditions used in the RELAP5 calculation to those used in the Westinghouse EM calculation. The results of the RELAP5 calculation are

presented in Section 6. Qualitative and quantitative comparisons to the EM analysis performed by Westinghouse under the guidelines of 10 CFR 50 are also presented in Section 6. Section 7 details the conclusions reached concerning the RELAP5 analysis and the comparisons made to the licensing analysis.

2. PLANT AND POSTULATED ACCIDENT DESCRIPTION

The RESAR-3S NSSS is a Westinghouse pressurized water reactor consisting of a pressure vessel and 4 separate coolant loops. The vessel contains 193 nuclear fuel assemblies, each containing 264 fuel rods in a 17 x 17 array. There are 61 full length control rods for reactor control. Each coolant loop consists of a vertical, single-stage, centrifugal pump; a Type F steam generator with Inconel tubes; auxiliary feedwater systems; a steam dump system; ECC systems; and the connecting piping. A pressurizer and associated surge line is attached to one loop.

The postulated accident is a 4 inch break at the location where the accumulator line is welded to the cold leg in a loop without the pressurizer. This corresponds to the most limiting small break in terms of highest peak cladding temperature, as presented in the RESAR-3S Reference Safety Analysis Report.[2] Depressurization of the primary system causes a reactor trip, steam dump actuation, auxiliary feedwater flow, and ECC system actuation. Loss of primary coolant through the break eventually caused approximately 75% voiding of the system, but no significant or prolonged heatup was calculated in the core. The calculation was terminated at 1870 s after 110 s of RHR injection during which system mass inventory increased rapidly.

3. COMPUTER CODE AND MODEL DESCRIPTION

The computer code chosen for the small break calculation was RELAP5/MOD1 Cycle 18 with updates. RELAP5/MOD1 is an advanced best estimate computer code developed at INEL for small break calculations. The code has the capability for modeling all systems in an NSSS required for small break calculations as well as an extensive control system package.

Features unique to RELAP5 include subcooled and two-phase nonequilibrium and nonhomogeneous choked flow models, horizontal stratified flow and stratified choked flow models, noncondensibles in the vapor phase, and a two-phase mechanistic abrupt area change model.[3] RELAP5 calculations have been compared to other code calculations[4] and to experimental data.[4-7] Conclusions of these assessment efforts show that RELAP5 is an appropriate computer code for calculating the trends of the phenomena occurring in small break transients.

The model used in this calculation consists of 150 volumes, 159 junctions, and 181 heat structures. Figure 1 shows a nodalization diagram of the model. Three of the four loops were lumped together as the intact loop and the broken loop was modeled separately. The length of corresponding components in each loop was the same, with the intact loop components having three times the volume and flow area of the broken loop components. The pressurizer surge line connects into the intact loop hot leg. Charging pumps, safety injection pumps, accumulators, and residual heat removal (RHR) pumps were modeled in each loop. The charging flow was injected directly into the cold leg. The safety injection and RHR flows were injected into the accumulator line which was connected to the cold leg upstream of the charging line connection. The break was located in the single loop at the same location as the accumulator line connection with the intent of modeling a crack in the weld of the accumulator line to cold leg connection. The flow area of the break was 0.08727 ft^2; the equivalent of a 4 inch diameter circular hole.

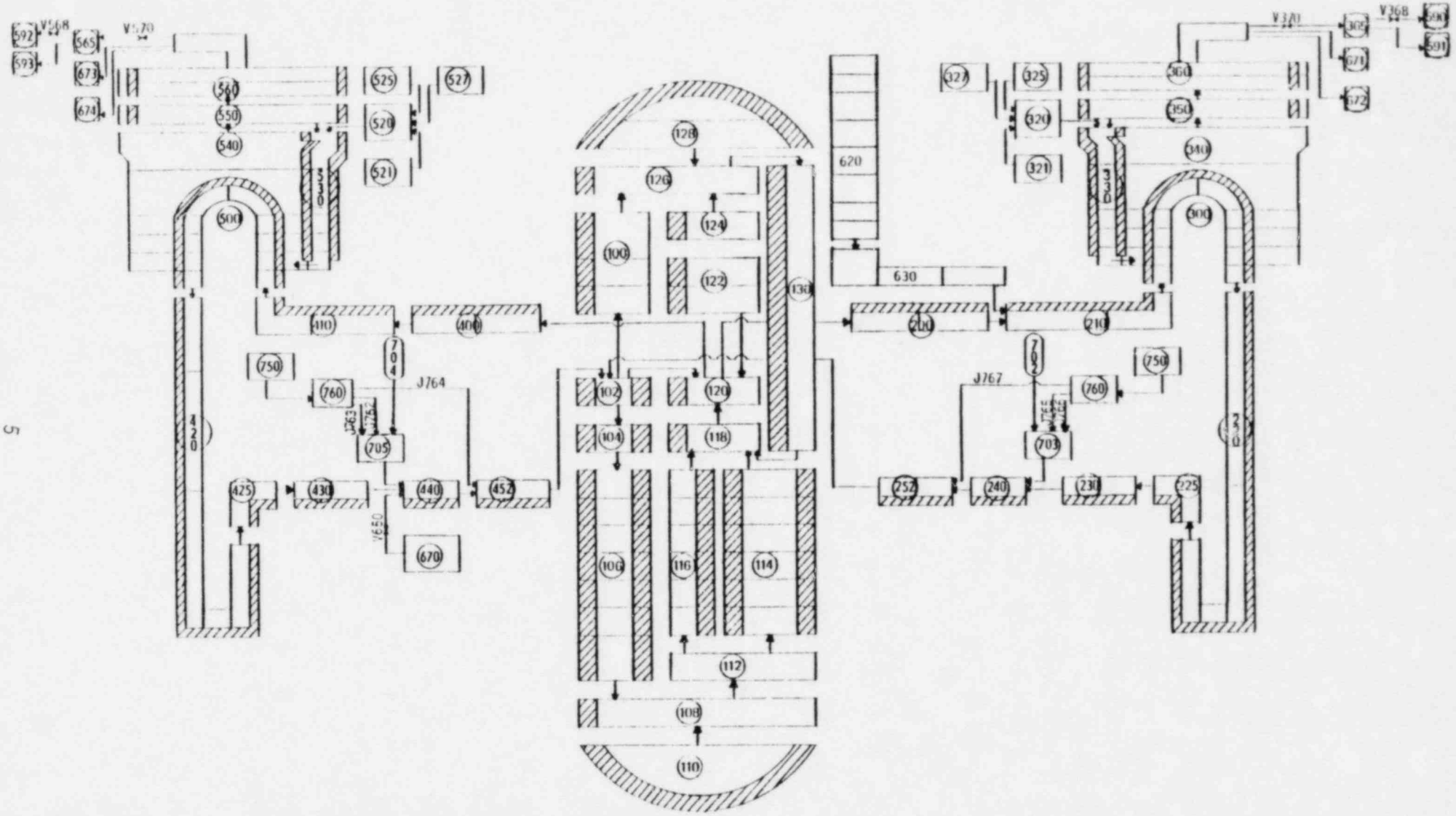

Figure 1. RELAP5 nodalization diagram for the RESAR-3S small break calculation.

The steam generator primary and secondary sides were modeled including internals metal mass and heat transfer area, main and auxiliary feedwater systems, steamline, relief valves, turbine stop valves, main steam isolation valves, and steam dump system. Since the RELAP5 separator component is an ideal separator (it allows only dry steam out the top) the steam separators and driers were lumped into one component. The steam dump system had the capability of relieving 40% of full load steam line flow. The atmospheric dump system and one of the spring loaded safety relief valves was modeled. More relief valves would have been added had they been needed for the calculation. The relief valves flow areas were sized to give the correct flow at the valve actuation pressure.

The reactor coolant pumps were modeled using PUMP components. Homologous curves, two-phase difference curves, and two-phase multiplier tables for head and torque for Westinghouse PWR pumps were used for all input requirements except the two-phase difference curves for the energy dissipation region of the head and torque curves. Semiscale two-phase difference data was the only information available to use for this input.

The pressurizer tank and surge line were modeled with PIPE components. Eight nodes were used in the pressurizer tank so the draining could be followed. The heaters and cooling spray were not modeled since they were not needed to reach steady state and would not be utilized in the transient. The power operated relief valve was not modeled since it would not be challenged in this transient.

The vessel model includes a downcomer, lower plenum, core region, core bypass, upper plenum, and upper head with an "inverted top hat." The model included the leakage path from the vessel inlet nozzles to the upper plenum, and the upper head spray nozzle flow path. The core region had six volumes so the liquid level could be tracked and the hydraulic conditions could be accurately calculated.

Heat structures were used to model the stored energy and heat transfer surfaces of the primary system loop piping; steam generator walls,

internals, and tubes; and vessel walls, internals, and fuel pins. One fuel pin was modeled as a hot pin, but there was no separate fluid volume for that pin. Heat losses to the ambient were not modeled. Heat transfer coefficients were calculated by the code for all heat structures except one in the vessel that was used to simulate gamma heating. This heat structure was modeled as a thin piece of steel with a large surface area and a high heat transfer coefficient so all the energy generated within it would be immediately transferred to the fluid in the vessel.

Other user selected code options include the following. Nitrogen was the noncondensible gas in the accumulator. Wall friction and unequal temperature options were implemented for all primary and secondary volumes except pumps and the steamline beyond the main steam isolation valves (MSIV). These options are not allowed for pumps. The main steamlines beyond the MISVs were not regions critical to the calculation so the options were chosen to minimize problems in achieving steady state conditions. With a few exceptions to be discussed later, the following modeling criteria were applied at the junctions. As recommended by the RELAP5 development group, choking was allowed at all junctions except at the separators; the geometry determined whether a junction had a smooth or abrupt area change; and the full inertia treatment option was selected for all junctions. Liquid and vapor could have unequal velocities except at the separator inlets and the accumulator line to cold leg connections. These selections gave more realistic void distributions in the steam generators and prevented problems that could occur by injecting cold water into a two phase system.

At 1522.2 s, a restart was performed which changed two upper head bypass flow junctions to mitigate a mass error problem. As suggested by the RELAP5 code development group, the junctions from the downcomer to the upper head and from the upper head to the guide tubes were given increased flow areas and loss coefficients. These changes would provide the same steady state flow through the junctions, but allow the code to calculate two-phase flow with less mass error. The choking and two velocity options were turned off for these junctions at this time. If this technique had been used for the entire calculation, the system mass error would have been

smaller but the system depressurization and core thermal hydraulics would not have been significantly altered.

Another restart was performed at 1722.2 s. The flow from a time dependent volume to the volume that feeds the pumped ECC trains was choking when RHR pumps came on. Since the area of this junction was arbitrarily chosen, it was increased to prevent the unrealistic choking problem. With these changes, the calculation ran smoothly to completion at 1870 s.

The updates used in this calculation include the following. One update fixes an error so that all restart variables are defined. Two updates cause the velocity term and mass terms in the momentum flux equation to be donored. Another update allowed mass error and total system mass to be used as minor edit and plot variables. At the 1722.2 s restart, an update was added to reduce the mass error. All updates were recommended by the code development group and are listed in Appendix A.

4. ASSUMPTIONS FOR BEST ESTIMATE AND EM CALCULATIONS

The assumptions for the initial and boundary conditions in the RELAP5 calculation are the result of getting best estimate conditions of a plant at typical operating conditions. Table 1 compares the assumptions used in the RELAP5 calculation to the assumptions used in the EM calculation. The conservatisms in the EM calculation are apparent in the lower ECC and auxiliary feedwater flow rates, longer delay times, higher water temperatures, and higher core power.

TABLE 1. COMPARISON OF ASSUMPTIONS USED IN THE RELAP5 BEST ESTIMATE CALCULATION AND THE EVALUATION MODEL CALCULATION

RELAP5	EM
ECC	
All trains working (2 safety injection pumps, 2 charging pumps, 2 RHR pumps)	One train working (one safety injection pump, one charging pump)
4 accumulators injecting into the primary system	3 accumulators injecting into the primary system
Pumped ECC is based on design head/flow curve with 10% of design head added uniformly over curve	Pumped ECC flow degraded 5% from design head
All ECC water at 90°F	Accumulator water at 120°F Pumped ECC water at 100°F
Safety injection delay = 10 s	Safety injection delay = 25 s
Steam Generator Secondary Side	
Steam dump system actuated at reactor trip	No steam dump system
2 motor driven auxiliary feedwater pumps, 500 gpm each, 30 s delay, 90°F water	1 motor driven auxiliary feedwater pump, 470 gpm, 60 s delay, 120° water
1 turbine driven auxiliary feedwater pump, 1000 gpm, 60 s delay, 90°F water	No turbine driven auxiliary feedwater pump
Core Power Decay	
76% of ANS + 20% power decay curve	ANS + 20% power decay curve
2.2 s rod drop time	3.4 s rod drop time
Total core power of 3411 Mw	Total core power of 3206.88 Mw
Total peaking factor of 1.678	Total peaking factor of 2.32
Reactor Coolant Pumps	
Tripped at 1300 psia	Tripped at 0 s

5. INITIAL AND BOUNDARY CONDITIONS

This section compares RELAP5 initial conditions to the desired initial conditions for a RESAR-3S plant. Differences between the boundary conditions of the RELAP5 best estimate calculation and the Westinghouse EM calculation are discussed.

5.1 Initial Conditions

When the model was assembled and quality assured (see Appendix B) the process of arriving at a steady state condition was initiated. The sum of the elevation changes of all flow loops was checked to ensure that all loops close. Estimates were made of initial fluid conditions throughout the system and these were applied to each volume. Estimates of mass flows were input for each junction. Power was applied to the core, the pumps were turned on to rated conditions, a time dependent volume was connected to the top of the pressurizer to force a constant pressure boundary condition on the primary side, main steam valves were opened, and feedwater was pumped into the steam generators. Feedwater flow was set equal to steam flow to maintain the desired secondary side inventory. A pump speed controller adjusted the pump speed to get the desired mass flow rate through the core. A steam valve controller adjusted the steam flow rate to get the correct cold leg temperature. The secondary side pressure had to be lowered by 61 psi below specified conditions and the recirculation flow ratio lowered to 3.1 from 3.7 to obtain a high enough heat removal from the primary to get the desired cold leg temperature.

Pressure drops around the system were compared with desired values and loss coefficients were changed to obtain desired pressure drops. Loss coefficients in the vessel bypass paths were adjusted to give correct flows in these areas.

The maximum stored energy in the fuel was determined from FRAPCON-2 runs (Appendix C) and a radial temperature profile was generated for the average and hot fuel pins. The radial temperature profile in the RELAP5 fuel pins was forced to match the FRAPCON-2 temperature profile. This procedure gave the correct stored energy in the fuel since the fuel properties and the fuel geometry were the same for both codes. The temperature profile in the RELAP5 model was changed by changing the gap conductance and fuel pellet radial power profile in an interative procedure with constant fluid conditions. Figure 2 compares the initial temperature profile used in RELAP5 to the desired (FRAPCON-2) temperature profile for the hot pin and average pins.

Steady state was reached when it was determined that selected pressures, temperatures, and flow rates were at their desired values and were not changing in time. Table 2 shows important system parameters at steady state conditions compared to desired conditions. After steady state was reached, the pump speed and steam valve position controllers were removed and those parameters were hold constant until conditions of the system during the transient dictated a change.

TABLE 2. INITIAL CONDITIONS

Parameter	RELAP5 Value	RESAR-3S Value
Cold leg temperature (°F)	557.7	557.6
Hot leg temperature (°F)	617.7	617.8
Pressurizer pressure (psia)	2255.	2250.
Primary coolant flow (lbm/s)	39091.	39111.
Total core power (MW)	3411.	3411.
Secondary side pressure (psia)	935.	1000.
Feedwater temperature (°F)	440.	440.
Steam mass flow rate (lbm/s)	1047.	1051.
Vessel ΔP (psi)	45.48	45.41
Steam generator ΔP (psi)	31.4	33.2

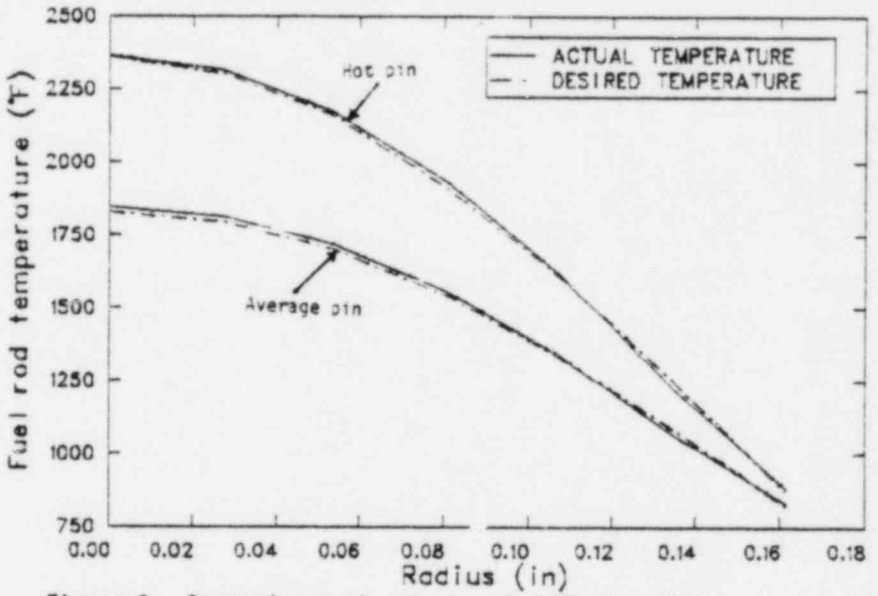

Figure 2. Comparisons of actual and desired radial temperature profiles for the hot and average fuel pins in the RELAP5 model.

5.2 Boundary Conditions

This section discusses the boundary conditions applied in the RELAP5 calculation, including fuel rod power, ECC injection parameters, and steam generator secondary side control. The setpoints and delays for the application of the boundary conditions are presented in Table 3. These boundary conditions are compared to the EM calculation boundary conditions where appropriate.

Heat losses to the environment were not modeled since they would be a negligibly small fraction of the system power during this calculation. The containment pressure was held constant at 14.7 psia throughout the calculation. The subcooled and two phase break flow multipliers were each set to 0.84 as recommended by the code development group and the LOFT program code users.

In both the RELAP5 and EM calculations, after the pressurizer pressure had dropped to 1860 psia there was a 2.0 s signal processing delay before a reactor trip signal was generated. From the time of the trip signal until the control rods were fully inserted was 2.2 s in the RELAP5 calculation and 3.4 s in the EM calculation. Reactor power did not begin to decay until the rods were fully inserted. A plot of the normalized power decay curve for both calculations is shown in Figure 3.

The reactor trip signal initiated the closing of the turbine stop valves which had a 0.5 s closing time. A steam dump system that directs up to 40% of the full power steamline flow directly to the condenser was enabled after the reactor trip signal was generated. The flow rate of the steam dump system was based on an average temperature that had been processed in a lead-lag controller. The lead time constant was 10 s and the lag time constant was 5 s. The EM calculation did not model a steam dump system.

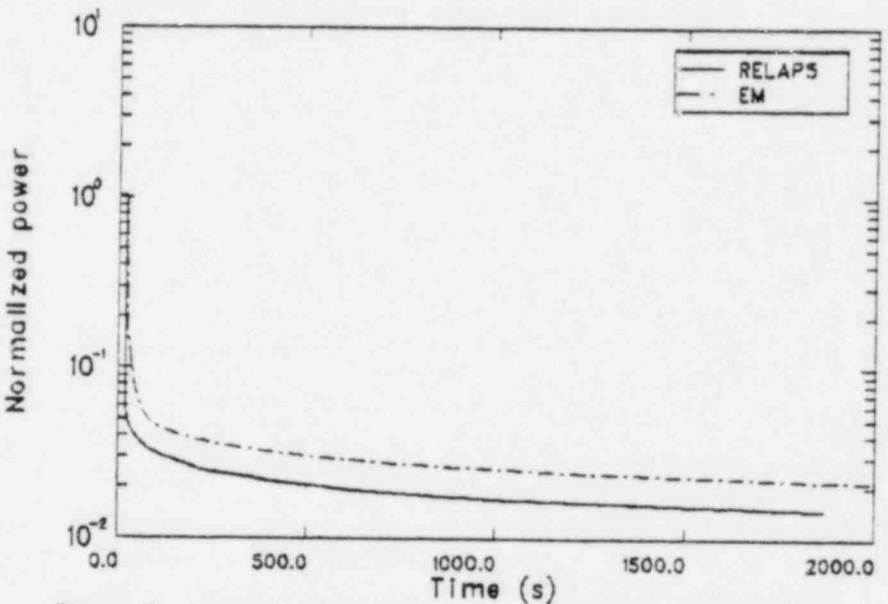

Figure 3. Comparison of normalized core power for RELAP5 and EM small break calculations.

TABLE 3. COMPARISON OF BOUNDARY CONDITION SETPOINTS FOR RELAP5 AND EM CALCULATIONS

Event	RELAP5 Setpoint[a] (Time Delay)	EM Setpoint (Time Delay)
Open break	time = 0.0 s	time = 0.0 s
Pressurizer low pressure	p = 1860 psia	p = 1860 psia
Close turbine stop valves	p = 1860 psia (2.0 s)	p = 1860 psia (2.0 s)
Begin power decay	p = 1860 psia (4.2 s)	p = 1860 psia (5.4 s)
Pressurizer low-low pressure	p = 1760 psia	p = 1760 psia[b]
Safety injection ("S") signal	p = 1760 psia (2.0 s)	p = 1760 psia[b] (2.0 s)
Charging flow initiated	"S" signal	"S" signal (25.0 s)
Close feedwater valve	"S" signal (2.0 s)	"S" signal
Safety injection flow initiated	"S" signal (10.0 s)	"S" signal (25.0 s)
Motor driven auxiliary feedwater flow started	"S" signal (30.0 s)	"S" signal (60.0 s)
Turbine driven auxiliary feedwater flow started	"S" signal (50.0 s)	N/A
Reactor coolant pumps tripped off	p = 1300. psia	time = 0.0 s
Accumulator pressure	600 psia	600 psia
RHR flow initiated	p = 215 psia	N/A

a. Time delay after setpoint is shown in parenthesis below the setpoint parameter.

b. Values obtained from Westinghouse data package for RESAR-3S plants.

A safety injection ("S") signal was generated 2.0 s after the pressurizer pressure reached 1760 psia. The main feedwater valves started closing 2.0 s after the "S" signal. In the RELAP5 calculation, the motor driven auxiliary feedwater pumps came on 30.0 s after the "S" signal, and the turbine driven auxiliary feedwater pumps came on 50.0 s after the "S" signal. In the EM calculation, the motor driven pump came on 60.0 s after the "S" signal. The auxiliary feedwater pumps were controlled to cover the steam generator tubes and keep them covered throughout the calculation without completely filling the generators.

In the RELAP5 calculation, the "S" signal initiated the pumped ECC injection with no delay for charging pump injection and a 10 s delay for safety injection pump actuation. In the EM calculation, no pumped ECC was injected until 25 s after the "S" signal. The accumulators were initiated at 600 psia and the flow rate was controlled by system pressure at the injection point for both calculations. RHR was ramped on from 200 to 215 psia in the RELAP5 calculation and was not considered in the EM calculation. Plots of pumped ECC flow rates vs. time are shown in Figure 4.

In the RELAP5 calculation, the reactor coolant pumps were tripped off at 1300 psia and allowed to coastdown. Reverse rotation was not allowed, but they were allowed to spin in a turbine mode. Reactor coolant pump speed is compared in Figure 5 for the RELAP5 and EM calculations. In the EM calculation, the pumps were tripped off at the initiation of the accident. Rated pump parameters used in the RELAP5 calculation are shown in Table 4.

TABLE 4. RATED PUMP PARAMETERS FOR RESAR-3S PUMPS

Speed (rpm)	1186.
Flow (gpm)	94400.
Head (ft)	304.
Torque (lbf-ft)	28015.
Moment of inertia ($lb\text{-}ft^2$)	95000.
Density (lbm/ft^3)	47.18

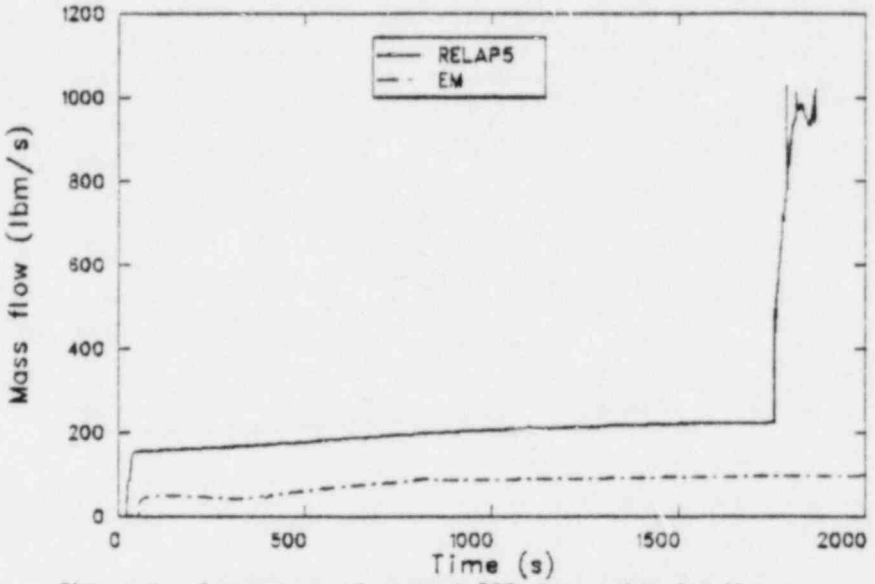

Figure 4. Comparison of pumped ECC flow rates for the RELAP5 and EM calculations.

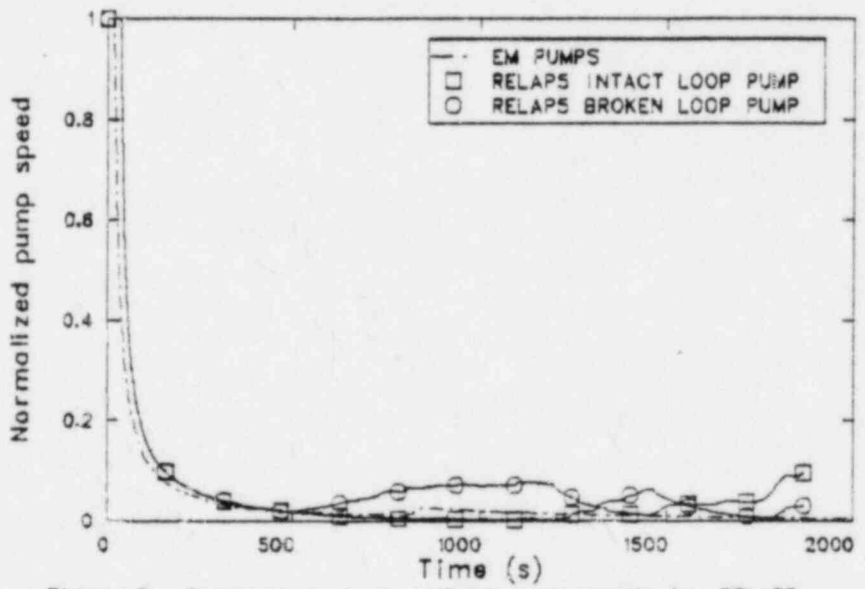

Figure 5. Comparison of normalized pump speeds for RELAP5 and EM calculations.

6. ANALYSIS RESULTS

The following two sections present the results of the analysis of the RELAP5 small break (i.e., 4 inch cold leg break) calculation for a RESAR-3S plant. The first section describes the general system behavior as calculated by the RELAP5/MOD1 program, and includes a detailed analysis of the factors which influenced the response. A brief summary of how the RELAP5 results compare with experimental data is also included in this section. The second section presents comparisons of results obtained from the RELAP5 calculation with the results obtained from the limiting small break calculation performed by Westinghouse for the RESAR-3S document. Comparisons are included in this section for each of the graphical outputs presented in the RESAR-3S document. These comparisons quantify the influence of the conservatisms imposed by 10 CFR 50.46 and Appendix K to 10 CFR 50 on the Westinghouse RESAR-3S calculation.

6.1 RELAP5 Calculation--General System Behavior

Table 5 presents a sequence of events highlighting important operations and thermal-hydraulic events which occur during a 4 inch cold leg break LOCA, as calculated by the RELAP5/MOD1 program. The system response to the small cold leg break is characterized by a continuous primary side depressurization, with only brief periods of dryout of the top third of the core. The periods of dryout occur just prior to blowout of the loop seal, and again after the initiation of accumulator flow.

Following the initiation of the transient, voiding of the primary system progresses from the upper elevations downward. The continued loss of fluid from the system via the break, in conjunction with the formation of liquid seals in the pump suction piping, causes a gradual depression of the mixture level in the vessel below the top of the core. The corresponding dryout of the upper portion of the fuel rods results in a limited rod temperature increase (temperatures remain less than steady state full power temperatures). However, blowout of the loop seal shortly after the core begins to uncover leads to a recovering of the core, and the

TABLE 5. SEQUENCE OF EVENTS FOR RELAP5 SMALL BREAK CALCULATION

Event	Time (s)
Blowdown initiated	0.0
Pressurizer low pressure trip setpoint (1860 psia) reached	15.2
Intact/broken loop turbine stop valves begin to close	15.3
Steam dump system actuated	15.3
Core power decay initiated	19.5
Pressurizer safety injection signal setpoint (1760 psia) reached	20.4
Charging pump flow initiated	22.5
Intact/broken loop main feedwater valves begin to close	24.5
High pressure injection pump flow initiated	32.5
Intact/broken loop pump coastdown initiated	34.9
Pressurizer emptied	40
Upper plenum/hot leg fluid saturates	38-42
Auxiliary feedwater flow initiated	52.6
Upper head begins to drain	200
Broken loop pump suction legs clear and break uncovers	520
Intact/broken loop accumulator injection initiated	858
RHR pumped injection initiated	1755
Calculation terminated	1870

mixture level remains above the top of the core until after accumulator injection begins. The accumulation of liquid in the pump suction piping after accumulator injection starts, results in two futher periods (again of brief duration) in which the mixture level in the vessel is depressed below the top of the core. Again, however, rod temperature increases are limited, and peak cladding surface temperatures remain well below the full power steady state temperatures. Once injection from the low head residual heat removal pumps begins, the rate of liquid addition to the primary system (via all active components of the ECC system) is sufficient to cause a rapid increase of the primary system liquid inventory, thus assuring adequate and continued cooling of the core.

The system thermal-hydraulic response is discussed in more detail in the following paragraphs, and the factors that influence the system behavior as the transient progresses are identified. System pressure response, system mass inventory/distribution, core thermal-hydraulic response, and break flow behavior (including the influence of ECC injection and break flow) are the primary phenomena of interest.

6.1.1 System Pressure Response

The vessel upper plenum pressure for the small break transient is shown in Figure 6. The timing of events which influence the depressurization rate are also indicated in the figure. Immediately following rupture, the primary system fluid (exclusive of the pressurizer fluid) is subcooled and the depressurization is rapid. By between 38 and 42 seconds, the system depressurizes to the saturation point of the fluid occupying the volume between the vessel upper plenum and the inlet plena of the steam generators, as indicated in Figures 7 and 8 which compare the vessel upper plenum and intact loop steam generator inlet plenum volume equilibrium temperatures with their corresponding volume saturation temperatures. Bulk boiling of the hot fluid at this point (beginning near the inlet of the steam generator and working its way back to the vessel upper plenum) is sufficient to slow the depressurization rate (Figure 6) as steam generation tends to offset the effect of coolant volume loss at the break. The system then continues to depressurize at a

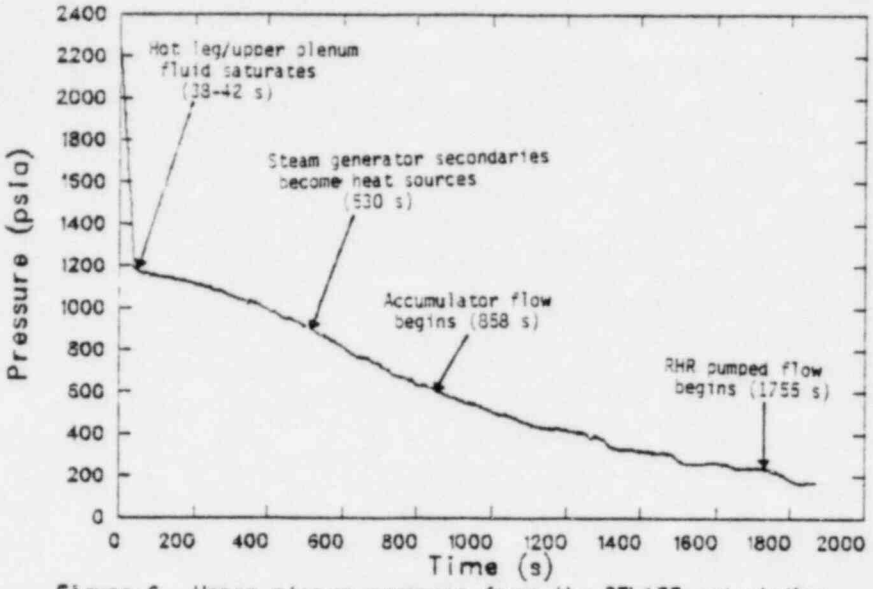

Figure 6. Upper plenum pressure from the RELAP5 calculation.

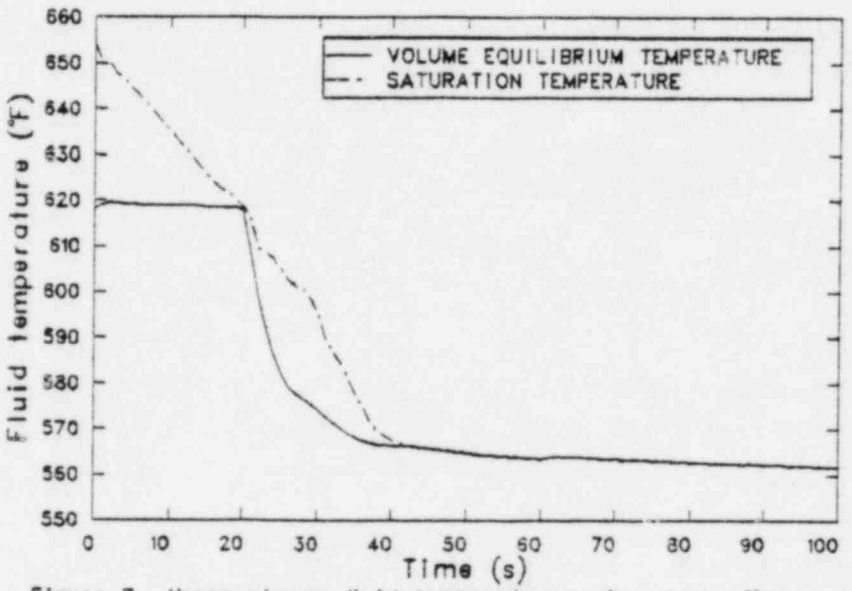

Figure 7. Upper plenum fluid temperature and corresponding saturation temperature from the RELAP5 calculation (0 TO 100 s).

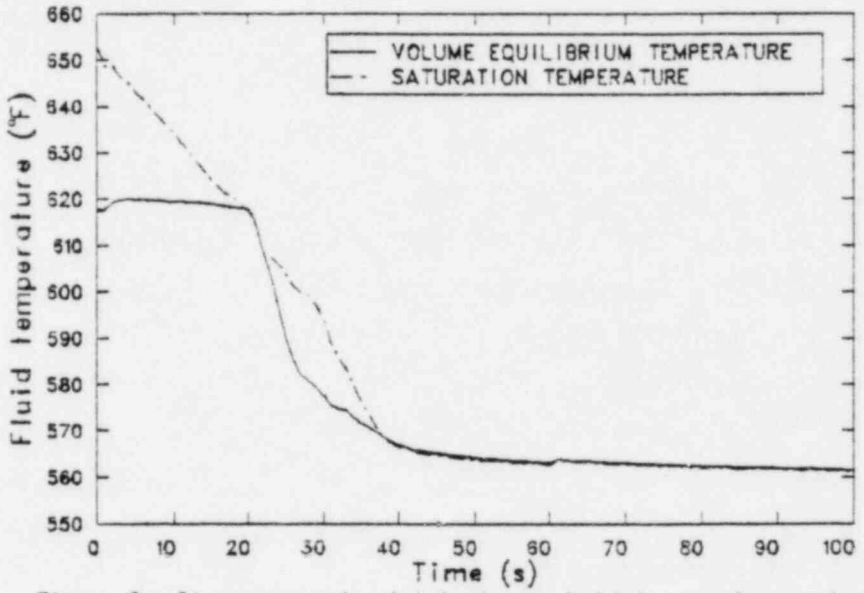

Figure 8. Steam generator inlet plenum fluid temperature and corresponding saturation temperature from the RELAP5 calculation (0 TO 100 s).

gradually increasing rate until between 530 and 590 seconds when the steam generator secondaries become a source of heat to the primary system. After this point, the system continues to depressurize but at a gradually decreasing rate of depressurization. During the accumulator injection period, the system depressurization exhibits a stepped response that is due to the combined effects of the accumulator injection, break flow, and loop hydraulic response. The mechanism for the stepped pressure response is discussed in more detail in Section 6.1.4. By 1755 seconds the system is depressurized to the point that allows ECC injection from the residual heat removal pumps to begin. The system continues to depressurize further through the termination of the calculation at 1870 seconds.

6.1.2 System Mass Inventory/Distribution

The primary system transient mass inventory for the small break calculation is shown in Figure 9. During the first 500 seconds (or prior to clearing of the loop seal), depletion of the primary system liquid inventory is quite rapid, as the system pressure is high and conditions in the break volume are primarily single phase liquid. Blowout of the loop seal at 520 seconds causes the fluid conditions in the break volume to change from single phase liquid to a relatively high void fraction liquid/steam mixture, which when combined with the steadily falling primary system pressure, results in a considerably reduced break flow rate and a leveling off of the system mass inventory. Accumulator injection (beginning at 858 seconds) initially results in a minor increase in system mass inventory, although a significant recovery of inventory is prevented because of the on/off nature of the accumulator flow and because of an increase in the break flow rate when subcooled ECC is present in the break volume (see Section 6.1.4). However, as the transient progresses, further reductions of the primary system mass inventory occur (between 1160 and 1325 seconds, and again between 1450 and 1750 seconds), even with the accumulators continuing to inject. These reductions in mass inventory occur as a result of the accumulation of liquid in the broken loop pump suction leg piping which leads to a significant increase in the subcooling of the liquid present in the break volume and a corresponding increase in the break flow rate. The loop hydraulics during these periods of increased system mass loss are discussed in more detail below. Initiation of liquid

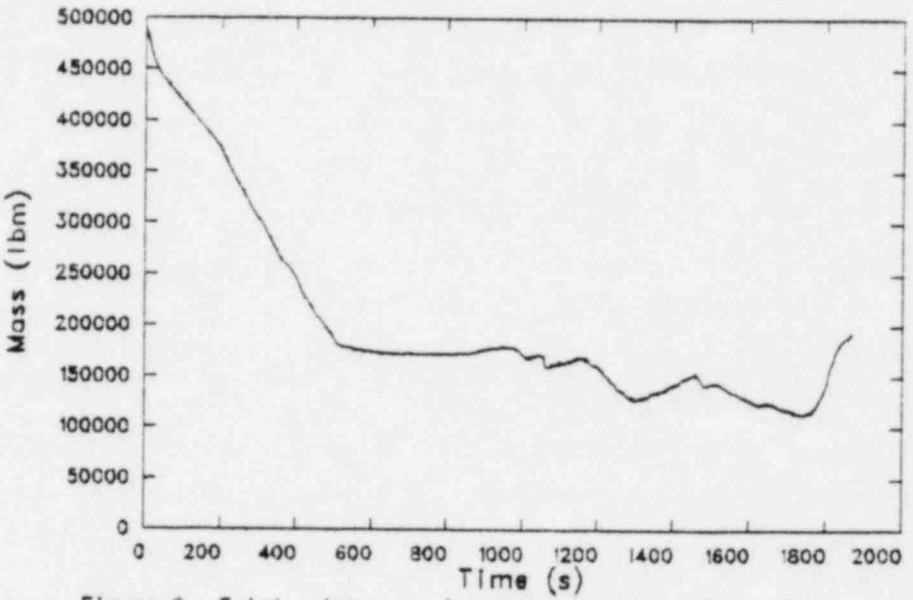

Figure 9. Total primary system mass inventory from the RELAP5 calculation.

injection from the residual heat removal pumps at 1755 seconds leads to a relatively rapid increase in the primary system mass as the combined ECC injection rate (from all components) becomes significantly greater than the break flow rate. The increase in mass inventory then continues through the termination of the calculation.

The primary system mass distribution for the small break calculation is characterized by the voiding of the upper elevations of the system, with liquid collecting in the lower elevations. Immediately following rupture, liquid lost out the break is made up by the liquid draining from the pressurizer, and the primary system remains essentially liquid solid. When the pressurizer has nearly emptied (i.e., at about 39 seconds), flashing of the hotter fluid in the primary system begins. Voiding of the primary system fluid occurs first on the upflow side of the intact loop steam generator (as fluid in the intact loop hot leg is at a slightly higher temperature than in the broken loop hot leg due to mixing with the hot pressurizer fluid), and then progresses through the remainder of the upper portions of the system as the transient continues. Figure 10 and 11 show the collapsed liquid levels in the upflow and downflow legs of the intact and broken loop steam generators, respectively. As indicated in Figure 10, voiding of the intact loop steam generator begins at about 40 seconds, and the upflow and downflow sides are essentially empty by about 450 and 350 seconds, respectively. Voiding of the broken loop steam generator (Figure 11) begins somewhat later (at about 60 seconds) and the upflow and downflow legs are emptied by about 440 and 300 seconds, respectively. Figure 12 shows the collapsed liquid level in the upper plenum portion of the vessel (covering the distance from the top of the core to the hot leg centerline), while Figures 13 and 14 show the void fraction in the intact and broken loop hot legs near the vessel. Again, each figure indicates a gradual depletion of liquid inventory beginning at about 60 seconds. Figure 15 compares the collapsed liquid levels in the downcomer and across the core, covering the region between the hot/cold leg centerline and the bottom of the core barrel. The downcomer remains essentially full until about 350 seconds. However, depletion of the core liquid begins at about 60 seconds and continues at a relatively constant rate until about 225 seconds. At this point a reversal of the core flow causes a sudden decrease in the core level, although the flow reversal also allows liquid

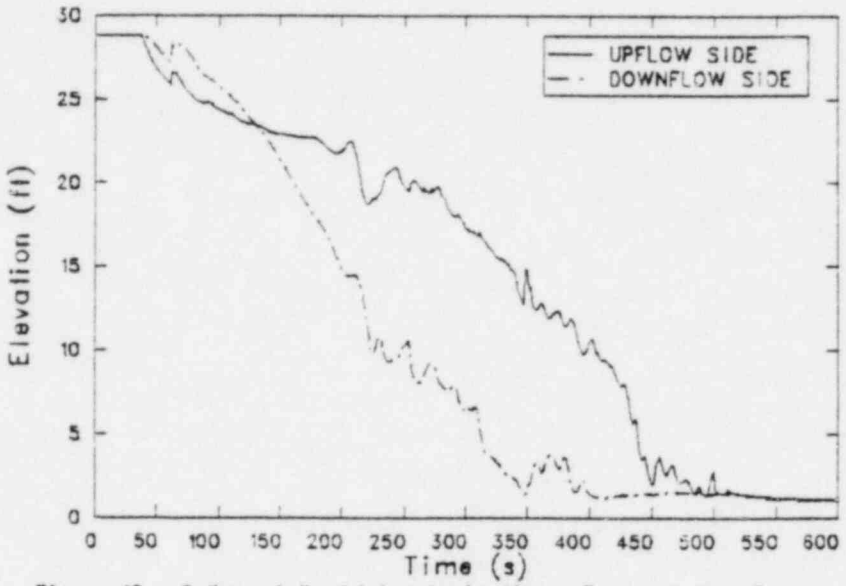

Figure 10. Collapsed liquid levels in the upflow and downflow sides of the intact loop steam generator tubes from the RELAP5 calculation (0 TO 600 s).

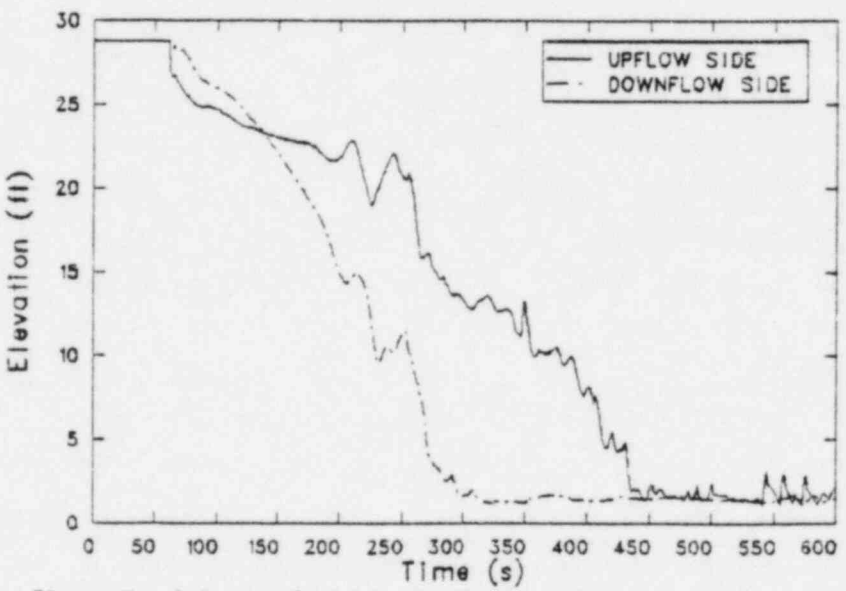

Figure 11. Collapsed liquid levels in the upflow and downflow sides of the broken loop steam generator tubes from the RELAP5 calculation (0 TO 600 s).

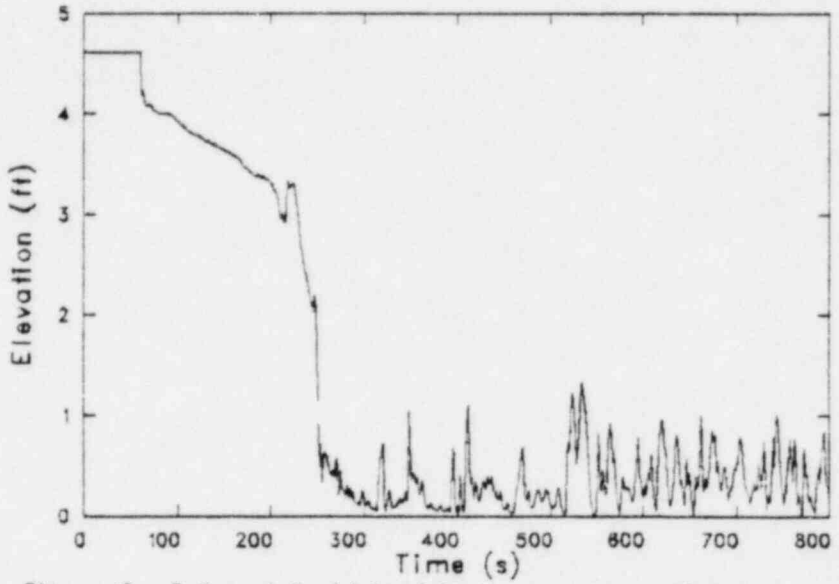

Figure 12. Collapsed liquid level in the core upper plenum from the RELAP5 calculation (0 TO 600 s).

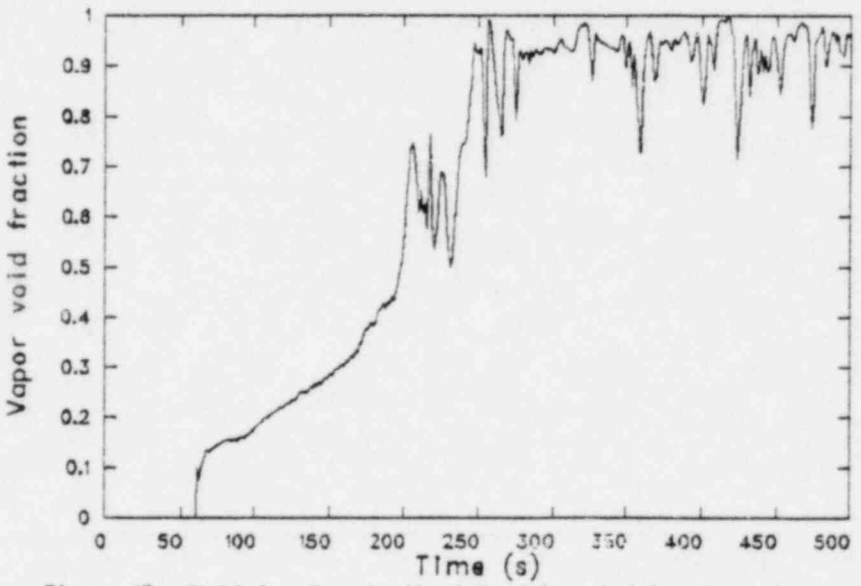

Figure 13. Void fraction in the intact loop hot leg from the RELAP5 calculation (0 TO 500 s).

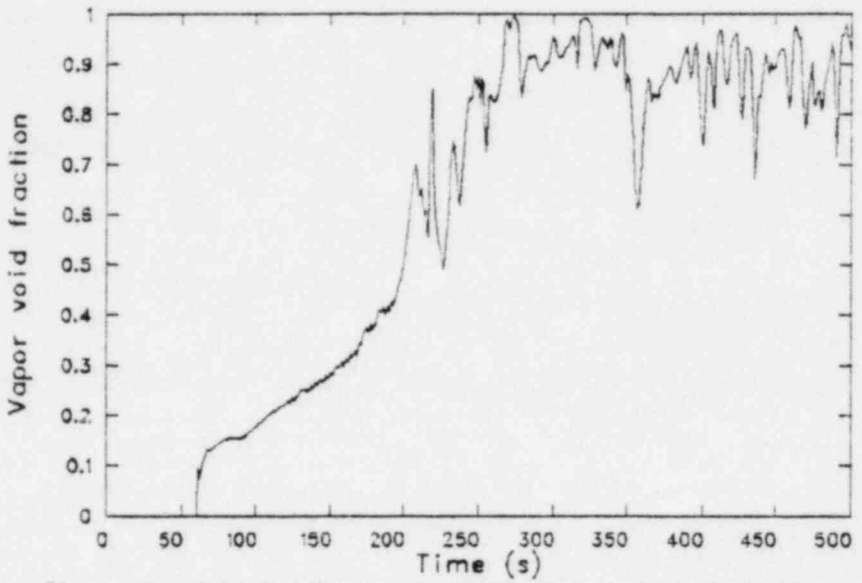

Figure 14. Void fraction in the broken loop hot leg from the RELAP5 calculation (0 TO 500 s).

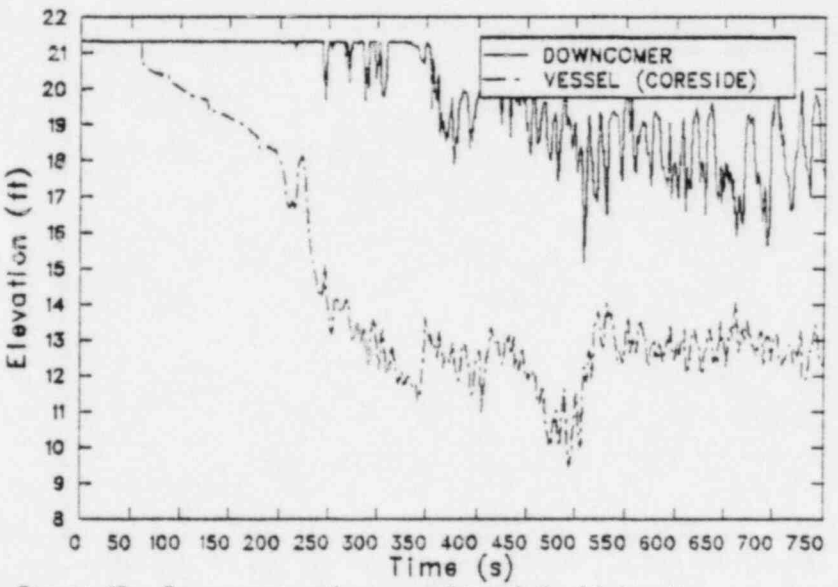

Figure 15. Downcomer and core collapsed liquid levels relative to the bottom of the core barrel from the RELAP5 calculation (0 TO 750 s).

in the upper portions of the system to begin to drain back into the vessel. Thus between 225 and 400 seconds, the rate of decrease of the core level is reduced as liquid from the upflow sides of the steam generators and from the upper head and guide tube volumes drains back into the upper plenum and core regions.

As the upper portions of the system empty, liquid in the pump suction piping forms seals which impede the flow of steam from the core region around the loops to the break. The resulting higher pressure in the core/upper plenum region, relative to the break location, causes a depression of the liquid levels in the downflow legs of both the intact and broken loop pump suction piping and in the core. Figures 16 and 17 compare the collapsed liquid levels in the upflow and downflow legs of the intact and broken loop pump suction, respectively, and show the decrease in the downflow leg liquid level below that of the upflow leg in both loops after about 400 seconds. Referring again to Figure 15, a further depression of the core liquid level occurs after about 410 seconds (i.e., once liquid stops draining back into the vessel from the high points of the system). The depression of the core liquid level at this time leads to an intermittent uncovering of the top of the core between about 450 and 520 seconds (see Section 6.1.3). However, by 520 seconds the liquid level in the broken loop pump suction downflow leg reaches the bottom of the suction piping, and a rapid clearing (blowout) of the liquid in the upflow leg then begins (see Figure 17). The resulting flow path through the broken loop from the vessel to the break allows equalization of the upper plenum/break region pressure, and a rapid increase in the core liquid level occurs (see Figure 15).

Between the blowout of the loop seal and about 1150 seconds, the core level remains relatively constant and the downcomer level exhibits a gradual increase as the combined ECC injection rate from all sources during this period is somewhat greater than the break flow rate. However, between 1160 and 1325 seconds and again between 1450 and 1750 seconds, the core level exhibits a significant decrease as indicated in Figure 18 which compares the long term downcomer and core levels. The core level depression during these periods is a result of the reformation of the loop

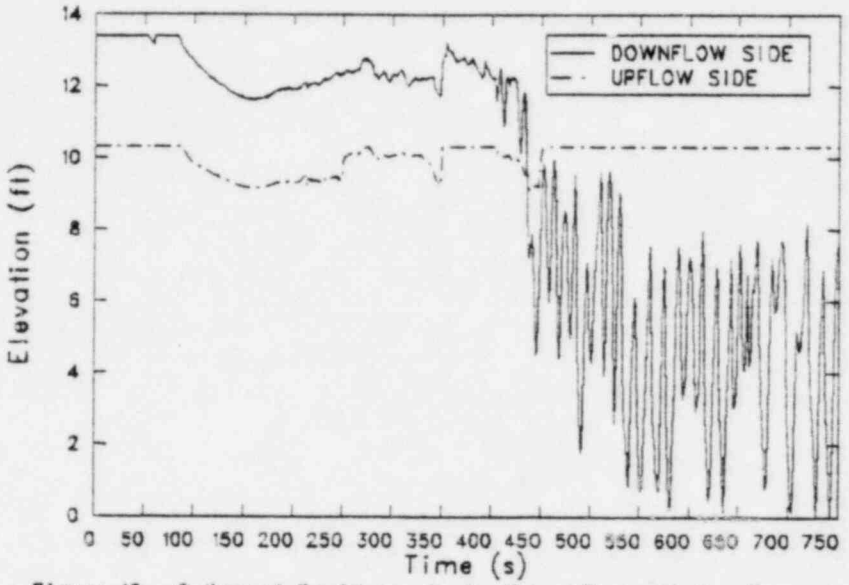

Figure 16. Collapsed liquid levels in the upflow and downflow sides of the intact loop pump suction from the RELAP5 calculation (0 TO 750 s).

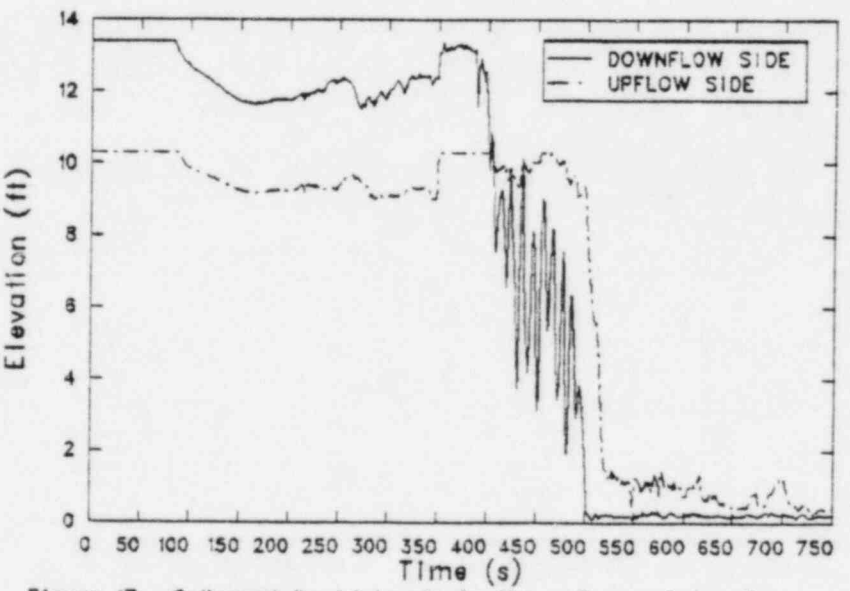

Figure 17. Collapsed liquid levels in the upflow and downflow sides of the broken loop pump suction from the RELAP5 calculation (0 TO 750 s).

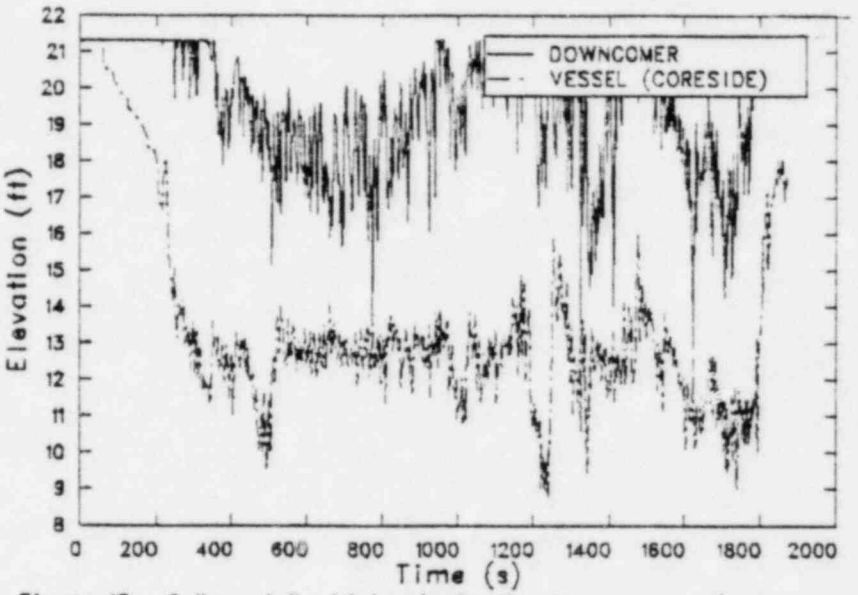

Figure 18. Collapsed liquid levels in the downcomer and core relative to the bottom of the core barrel from the RELAP5 calculation.

seal. Figure 19 compares the collapsed liquid levels in the upflow and downflow legs of the broken loop pump suction piping and illustrates the presence of the seal during the periods of level depression in the core. The depression of the core liquid level during these periods again results in an intermittent dryout of the top of the core, although temperature increases are limited. Referring again to Figure 18, a rapid increase in both the downcomer and core levels occurs once injection from the low head residual heat removal pumps begins at about 1755 seconds.

6.1.3 Core Thermal/Hydraulic Responses

The vessel liquid inventory for the small break calculation remains sufficiently high that the rod cladding temperatures stay below the steady state full power cladding temperatures throughout the transient, although as indicated previously, there are brief periods when dryout of the upper portion of the core leads to minor cladding temperature increases. Figures 20 and 21 show the rod cladding temperatures at the 10 to 12 and 8 to 10 foot elevations above the bottom of the core, respectively, for an average power rod, while Figures 22 and 23 show the cladding temperatures at the same elevations for the hot pin. Except for the period between 320 and 520 seconds and again between 1200 and 1250 seconds, and 1670 and 1740 seconds when intermittent dryout of the top third of the core gives rise to cladding temperature increases of a maximum of about 30 degrees Farenheit, the cladding temperatures generally remain a few degrees above the fluid saturation temperature. Figure 24 shows the cladding temperature on the hot pin at the 6 to 8 foot level above the bottom of the core, and does not indicate any rod dryout at this elevation.

The factors which influenced the hydraulic response of the core are indicated on Figure 25 which shows the collapsed liquid level in the core covering the active fuel region. As the system depressurizes following rupture, boiling of fluid in the core causes the initial decrease in core liquid inventory shown in Figure 25. Figure 26 compares the vapor void fraction at different elevations in the core, and indicates the onset of boiling starting at about 60 seconds at the top of the core and progressing to the bottom of the core by about 229 seconds. By 225 seconds, the

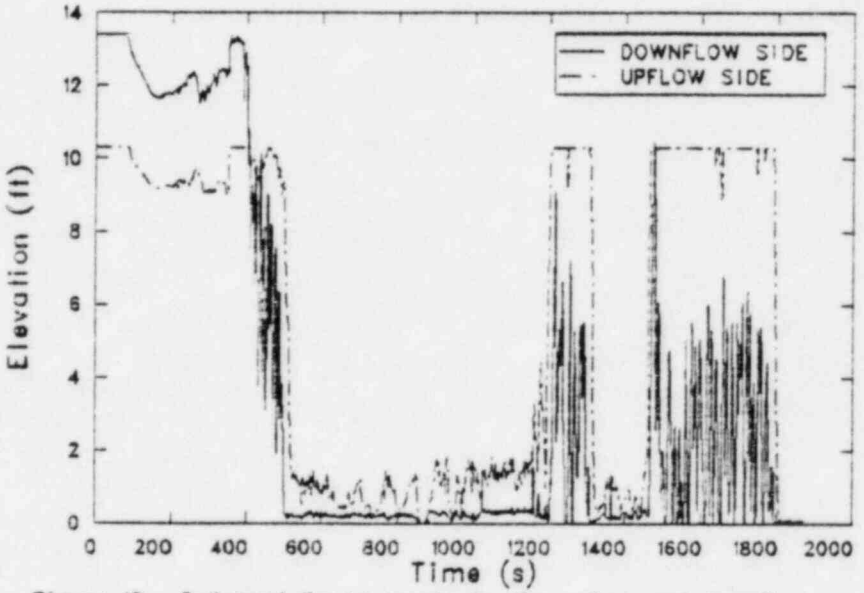

Figure 19. Collapsed liquid levels in the upflow and downflow sides of the broken loop pump suction from the RELAP5 calculation.

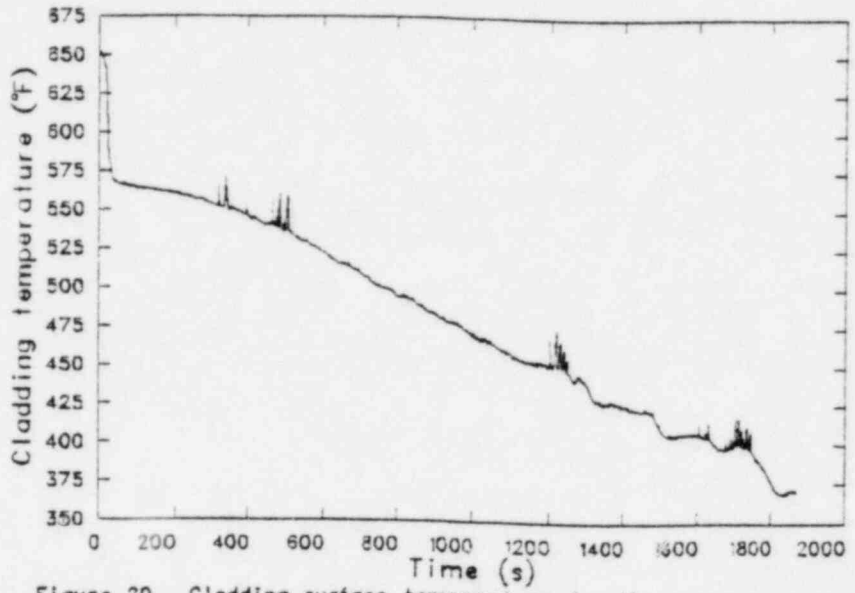

Figure 20. Cladding surface temperature for the average power fuel pins at the 10 to 12 foot elevation from the RELAP5 calculation.

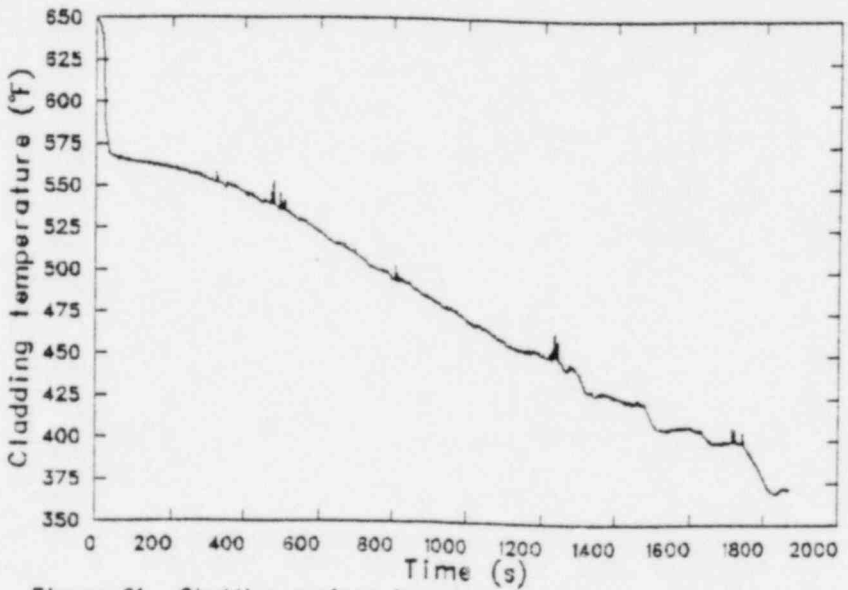

Figure 21. Cladding surface temperature for the average power fuel pins at the 8 to 10 foot elevation from the RELAP5 calculation.

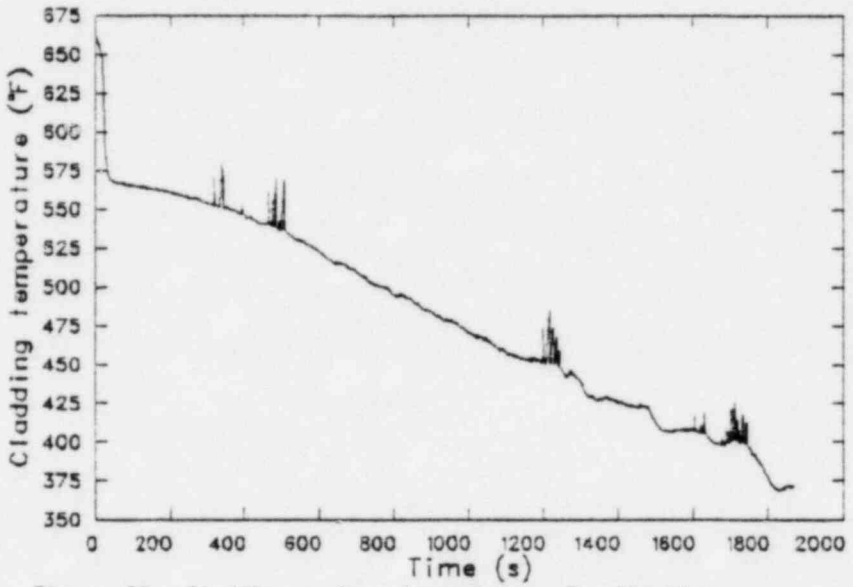

Figure 22. Cladding surface temperature for the high power fuel pin at the 10 to 12 foot elevation from the RELAP5 calculation.

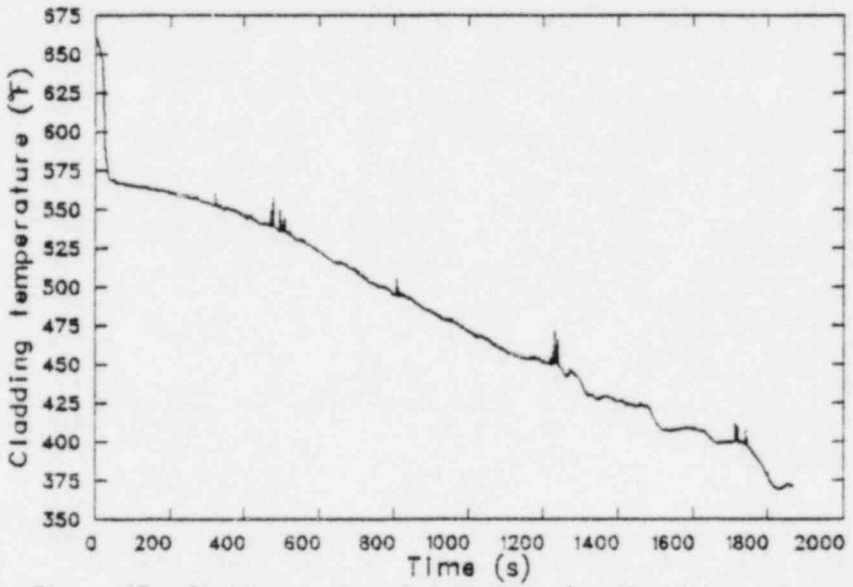

Figure 23. Cladding surface temperature for the high power fuel pin at the 8 to 10 foot elevation from the RELAP5 calculation.

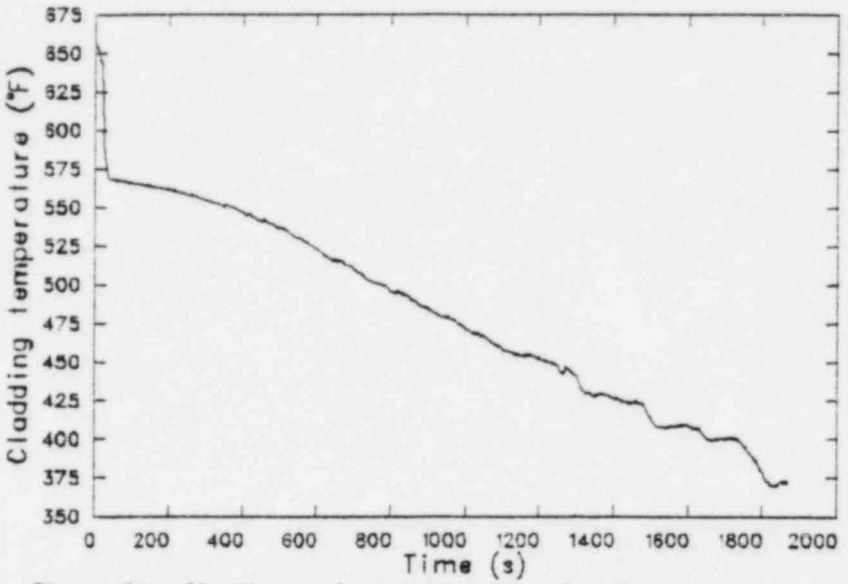

Figure 24. Cladding surface temperature for the high power fuel pin at the 6 to 8 foot elevation from the RELAP5 calculation.

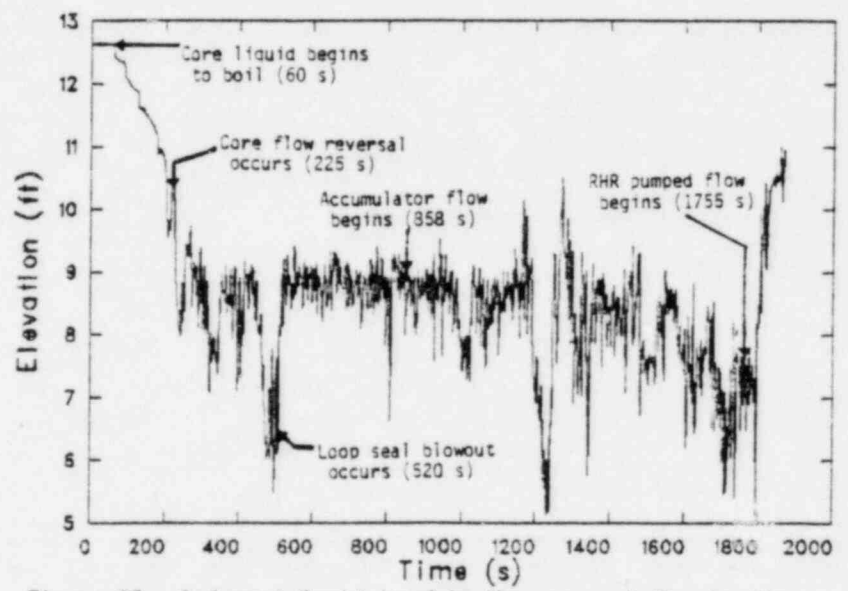

Figure 25. Collapsed liquid level in the core relative to the bottom of the active fuel from the RELAP5 calculation.

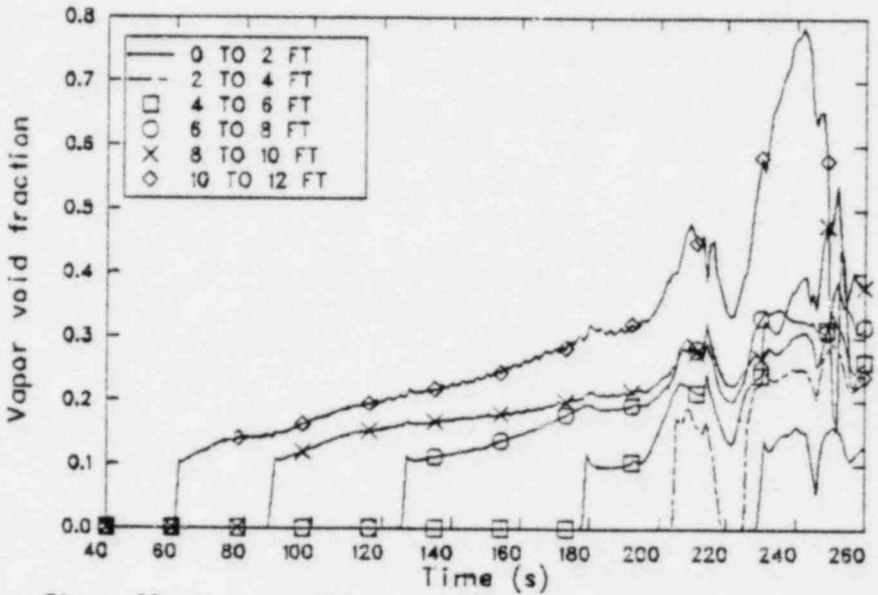

Figure 26. Void fraction in the core for the six volumes encompassing the active fuel region from the RELAP5 calculation (40 to 260 s)

effective head of the primary coolant pumps is reduced sufficiently (pump coastdown begins at 35 seconds) to allow reversal of core flow. At this point, fluid in the upper parts of the system (i.e., in the upflow sides of the steam generators and in the hot legs) begins to drain back into the vessel upper plenum and core regions. In addition, fluid in the vessel upper head becomes saturated at about 210 seconds, and also begins to drain into the upper plenum region. Figure 27 which compares the flow rate at the inlet to the core with the core collapsed liquid level, indicates an increase in level shortly after the core flow reversal occurs, followed by a period (lasting until about 430 seconds) when the liquid depletion rate is greatly reduced. By 430 seconds, most of the liquid in the upper parts of the system is depleted, and the core inventory once again begins to decrease as boiloff, combined with the presence of the loop seals (discussed earlier) causes a depression of the vessel/core liquid level. Figure 28, which compares the cladding temperature of the hot pin at the top of the core (10 to 12 foot elevation) with the vapor void fraction of the adjacent volume, shows the effect of the resulting dryout on the cladding temperature as the mixture level is depressed below the top of the core. The oscillatory nature of the core level at this point, however, causes the cladding to rewet shortly after each dryout, thus limiting the magnitude of the temperature increase. This period of dryout is terminated at 520 seconds by blowout of the loop seal, which leads to a rapid increase of the core liquid level (Figure 25) as liquid in the pump suction and cold leg piping is redistributed to the vessel.

As indicated previously, the period of dryout between 1200 and 1250 seconds is a result of the gradual accumulation of liquid in the broken loop pump suction piping which leads to a depression of the mixture level below the top of the core. Figure 29 compares the collapsed liquid levels in the upflow leg of the intact and broken loop pump suction piping and include the collapsed liquid level in the core. As shown in the figure, the liquid level in the broken loop pump suction begins to increase at about 1150 seconds (due to liquid draining back into the suction piping through the pump). As the level continues to increase, the flow path between the vessel upper plenum and the break (through the broken loop) becomes blocked and a reduction of the core level occurs. (Note that the

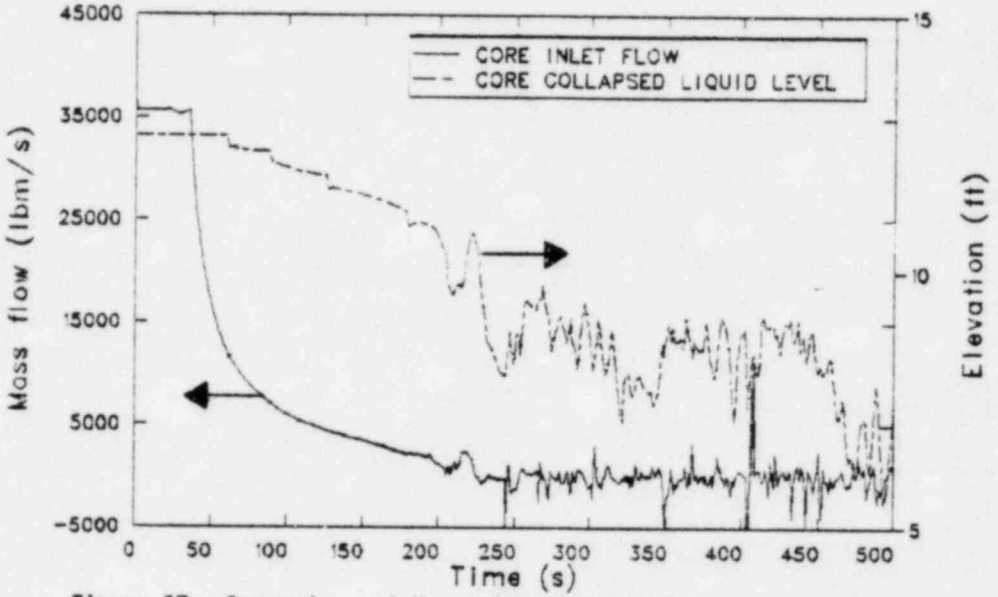

Figure 27. Comparison of the collapsed liquid level in the core region to the mass flow into the bottom of the core from relap5 calculation (0 to 500 s)

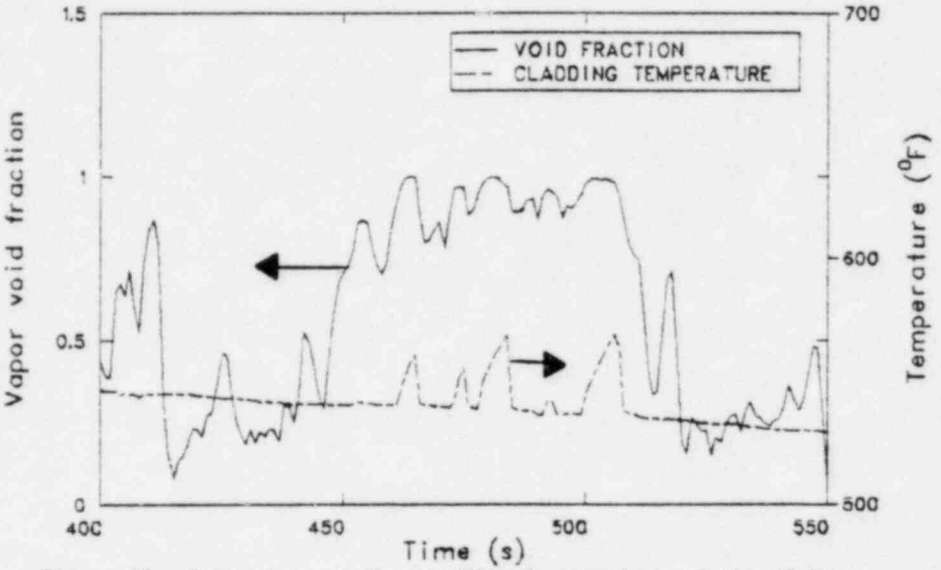

Figure 28. Comparison of the cladding temperature at top of the high power fuel pin to the void fraction at the top of the core from the RELAP5 (400 to 550 s)

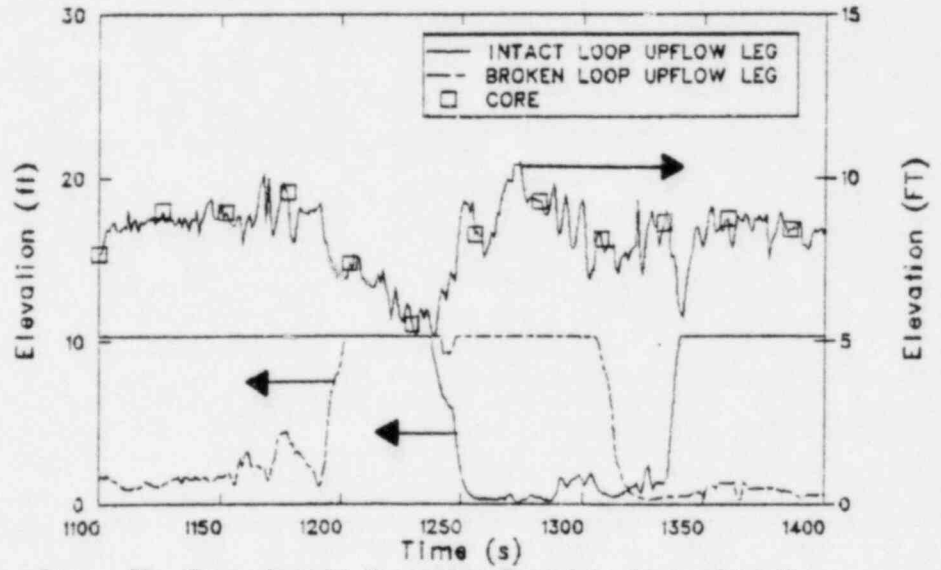

Figure 29. Comparison of the core collapsed liquid level to the collapsed liquid levels in the broken and intact loop pump suctions from the RELAP5 calculation (1100 to 1400 s)

intact loop pump suction has remained blocked with liquid since the beginning of the transient.) The reduction in core level is terminated at about 1240 seconds when liquid in the intact loop pump suction begins to clear. Figure 30 compares the rod cladding temperature of the hot pin at the 10 to 12 foot elevation above the bottom of the core with the void fraction of the adjacent fluid volume, and illustrates the cladding temperature increase which occurs as the volume becomes voided. Again, the cladding temperature increase is limited by rewet resulting from the oscillatory nature of the core liquid level.

The period of dryout between 1670 and 1740 seconds is once more a result of accumulation of liquid in the broken loop pump suction, but the dryout is not caused by a blockage of the steam flow paths around the loops as occurred earlier. Figure 31 compares the collapsed liquid levels in the upflow legs of the intact and broken loop pump suction piping, and again includes the core collapsed liquid level. As indicated in the figure, the liquid level in the broken loop suction upflow leg begins to increase at about 1450 seconds, and the leg is full by 1465 seconds. However, the intact loop suction leg begins to clear shortly after the broken loop leg begins to fill. (The intact loop suction leg piping refilled previously at about 1340 seconds--see Figure 29.) Thus a path for steam flow from the vessel to the break is maintained and the depression of the core level is miminal. The effect of blockage of the broken loop pump suction piping, however, is to cause an increase in flow rate from the vessel toward the break, which in turn causes a considerable increase in the degree of fluid subcooling in the break volume as cool ECC liquid is carried toward the break. As a result, a corresponding increase in the break flow rate occurs which leads to the further gradual depletion of the vessel inventory shown in Figure 31, and the intermittent dryout of the top third of the core between 1670 and 1740 seconds. Figure 32 compares the cladding temperature of the hot pin at the top of the core with the void fraction of the adjacent volume, and again illustrates the effect of the dryout. The reduction in core level is terminated once RHR pumped injection begins at about 1760 seconds, and a further rapid increase in the core level occurs at about 1790 seconds as the broken loop pump suction piping clears for a final time.

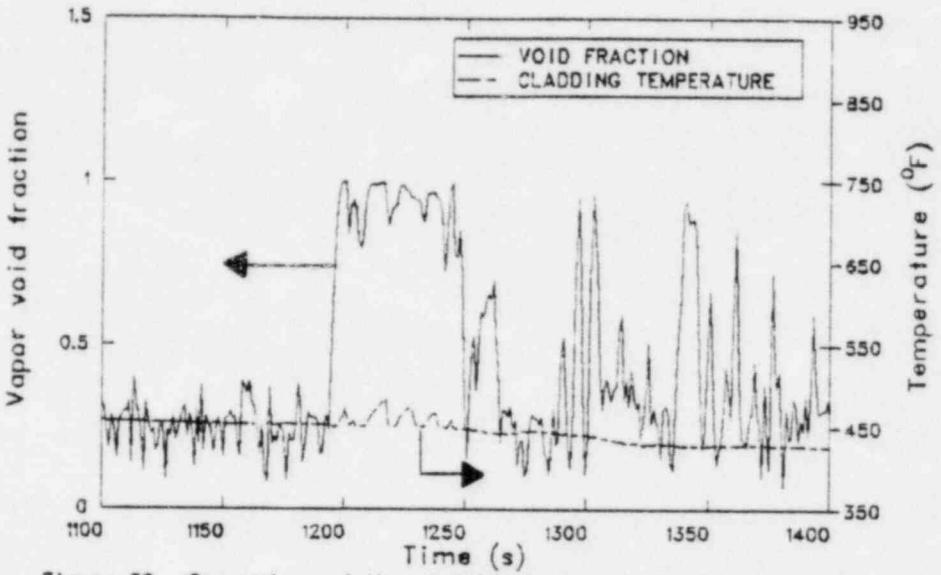

Figure 30. Comparison of the cladding temperature at the top of the high power fuel pin to the void fraction at the top of the core from the RELAP5 calculation (1100 to 1400 s)

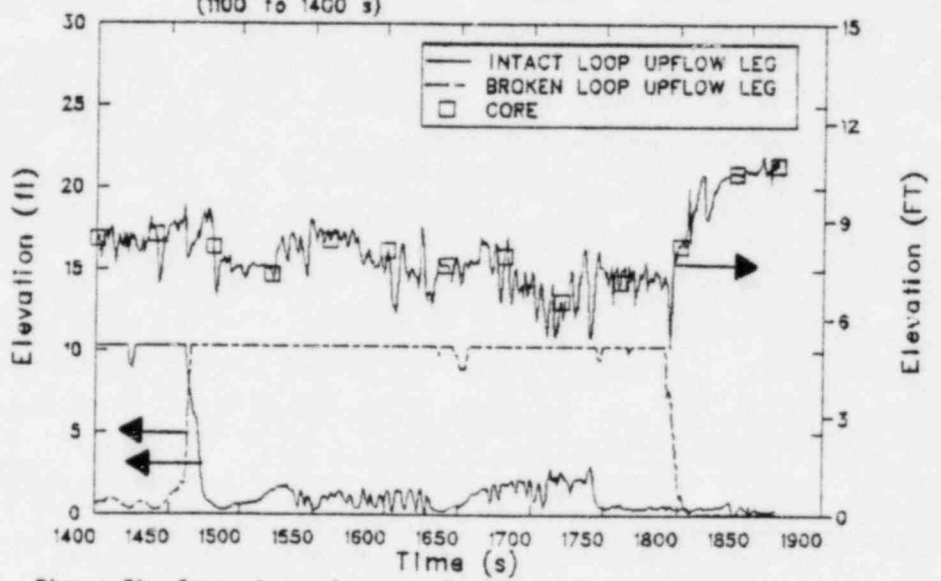

Figure 31. Comparison of core collapsed liquid level to the collapsed liquid levels in the broken and intact loop pump suctions from the RELAP5 calculation (1400 to 1900 s)

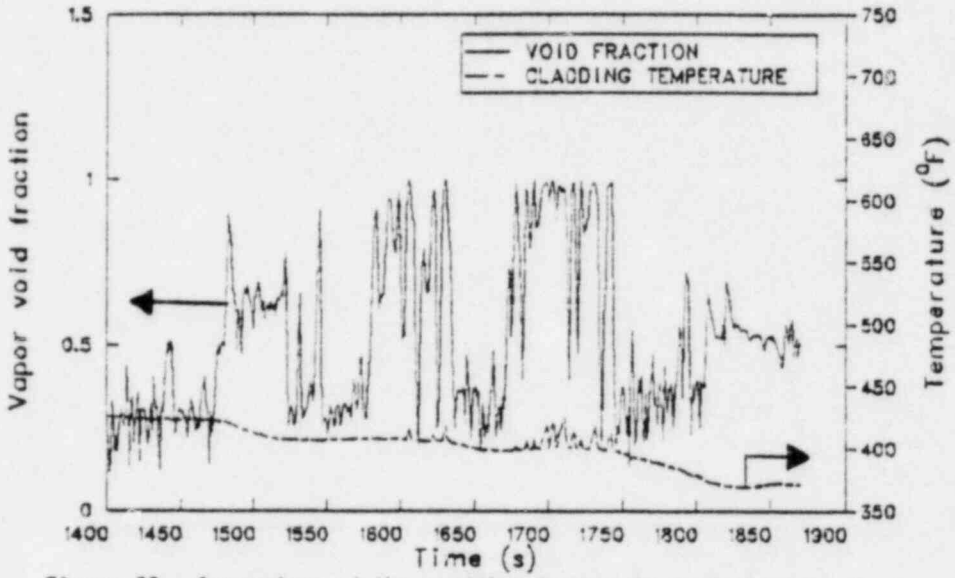

Figure 32. Comparison of the cladding temperature at the top of high power fuel pin to the void fraction at the top of the core from the RELAP5 calcation (1400 to 1900 s)

6.1.4 Break Flow Response

The break flow response for the small break calculation is shown in Figure 33. Following rupture, conditions in the break volume are single phase liquid, and the break flow decreases from its maximum just after rupture with decreasing primary system pressure. The slowdown in the primary system depressurization rate once flashing begins in the hot portions of the system (i.e., at about 40 seconds), causes the break flow to level off and remain fairly constant until about 190 seconds. By 190 seconds, the rate at which liquid is being supplied to the break volume by the broken loop pump falls below the break flow rate, and a flow reversal occurs in the piping between the break volume and the vessel. The flow reversal at this point is indicated in Figure 34 which shows the junction mass flow rate on the vessel side of the break volume. The effect of the flow reversal is to carry cool ECC liquid back into the break volume, thus supplying the break with relatively low enthalpy fluid which causes a corresponding increase in the break flow rate. Figure 35 compares the break flow rate with the break volume equilibrium fluid temperature, and shows the increase in break flow rate as the temperature decreases. The break flow rate remains relatively high (under the influence of the ECC liquid being injected into the cold leg piping) until blowout of the loop seal begins around 500 seconds. At this time, conditions in the break volume change from primarily single phase liquid to a relatively high void fraction mixture as the liquid is swept away from the break into the vessel. The change to high void fraction conditions in the break volume causes a corresponding reduction in the break flow rate as shown in Figure 36 which compares the break volume void fraction with the break flow rate. The break flow then remains relatively low until the initiation of accumulator injection (at about 858 seconds). The injection of accumulator liquid into the cold leg piping once again provides low enthalpy fluid to the break volume giving rise to an increase in break flow. Figure 37 compares the break flow rate with the break volume fluid equilibrium temperature (for a period after accumulator injection begins), and again illustrates the increase in break flow rate with a corresponding decrease in fluid temperature, and vice versa. The cyclic nature of the break flow response during the accumulator injection period is due to the oscillatory

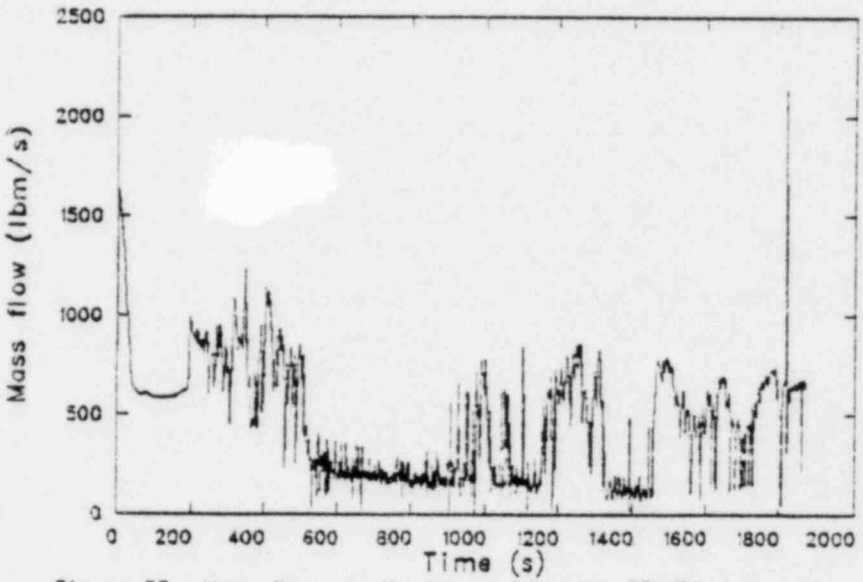

Figure 33. Mass flow out the break from the RELAP5 calculation.

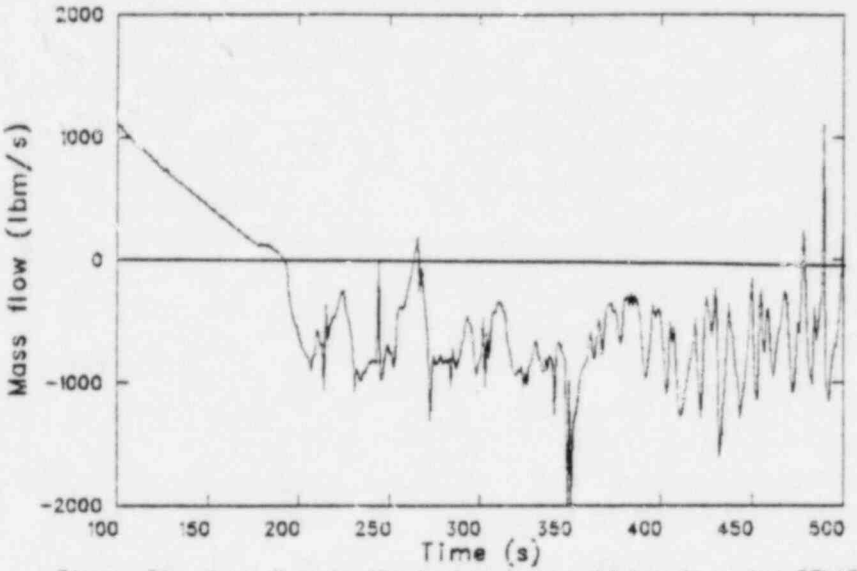

Figure 34. Mass flow in the broken loop cold leg from the RELAP5 calculation (100 to 500 s).

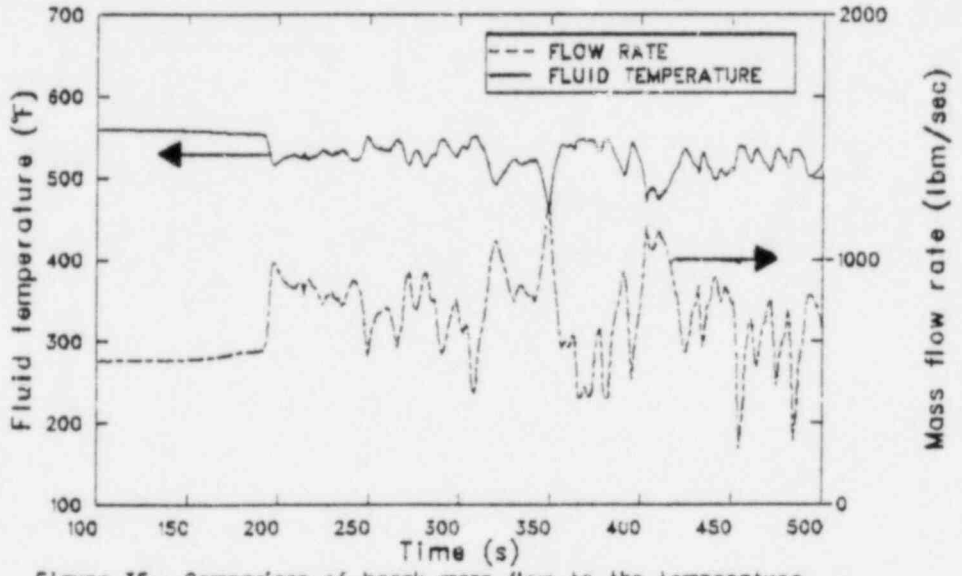

Figure 35. Comparison of break mass flow to the temperature of the fluid in the break volume from the RELAP5 calculation (100 to 500 s).

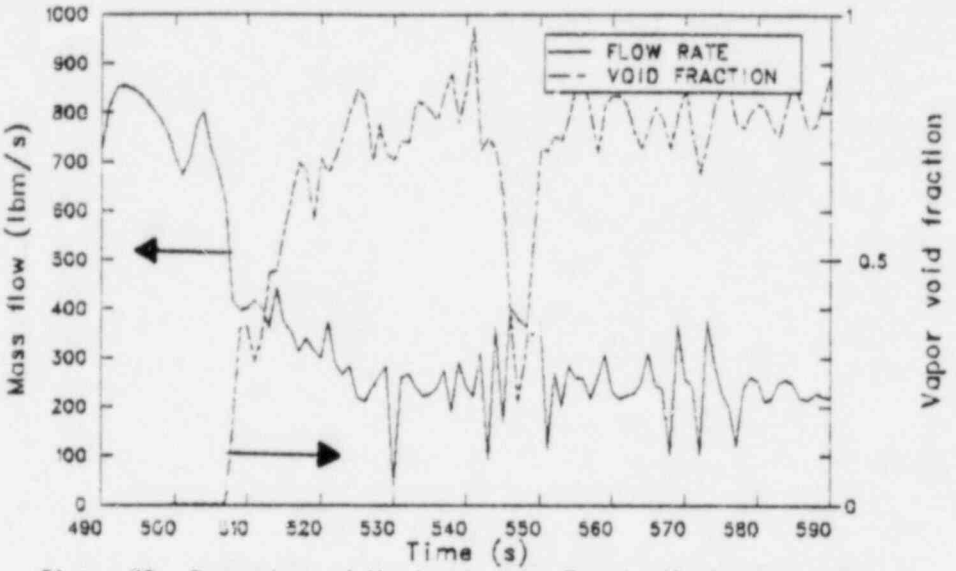

Figure 36. Comparison of the break mass flow to the break volume void fraction from the RELAP5 calculation (490 to 590 s)

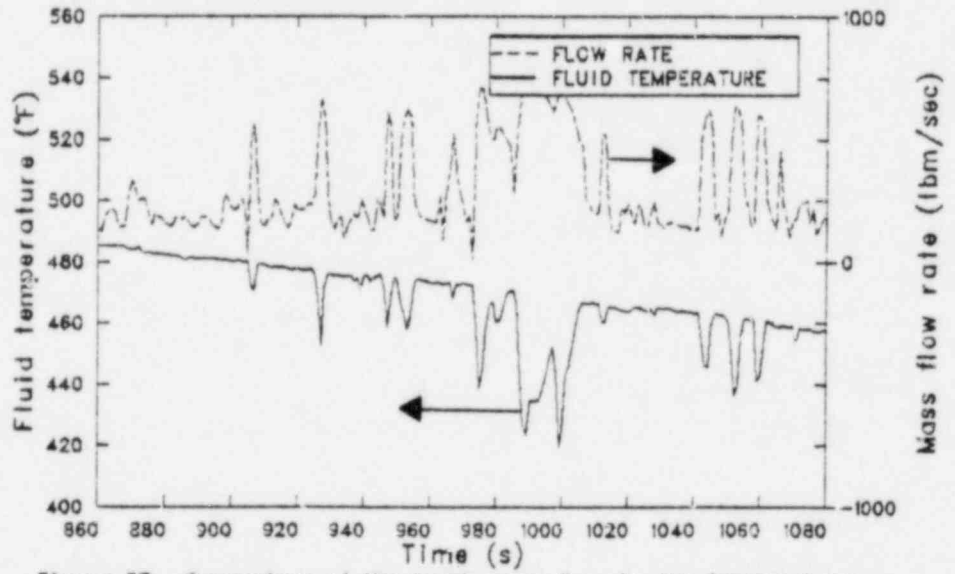

Figure 37. Comparison of the break mass flow to the temperature of the fluid flowing to the break from the RELAP5 calculation (860 to 1080 s).

flow in the piping between the vessel and the break volume. Figure 38 compares the break flow rate with the flow rate on the vessel side of the break volume. The figure shows that when flow is back into the break volume (i.e., negative loop flow), the break flow tends to be high as cool ECC liquid is being carried toward the break. Likewise when flow is out of the break volume toward the vessel (i.e., positive loop flow), the break flow tends to be low since the cool ECC liquid is then being carried away from the break.

Referring again to Figure 33, the break flow rate increases considerably during the periods between 1160 and 1325 seconds, and between 1450 seconds and the termination of the calculation. As discussed earlier, the broken loop pump suction piping during these periods is blocked by liquid (Figure 19), and the flow direction in the broken loop cold leg piping is directed primarily from the vessel toward the break. Figure 39 shows the mass flow rate on the vessel side of the break volume and indicates the relatively strong flow back into the break volume from the vessel. The net effect of the flow into the break volume is to supply the break with fluid that is as much as 100 degrees subcooled, as shown in Figure 40 which compares the break volume fluid temperature with the corresponding volume saturation temperature. This large degree of subcooling in the break volume gives rise to the high break flow rates indicated in Figure 33. The break flow rate decreases from these high values only after blowout of the broken loop pump suction piping once again allows the cold ECC fluid to be carried away from the break (i.e., toward the vessel).

6.1.5 Similarity of RELAP5 Calculation to Experimental Results

The experimental basis for evaluating how representative the RELAP5 small break calculation results are relative to "expected system behavior" includes many small break experiments conducted in the LOFT and Semiscale test facilities. Particular experiments which were similar in nature to the RELAP5 small break transient discussed herein include (but are not necessarily limited to) LOFT Test L3-5[8] and Semiscale Tests S-SB-2[9] and S-UT-4.[10] Each of these experiments simulated the rupture of a 4-inch pipe in the cold leg of a PWR, although boundary conditions (such as ECC

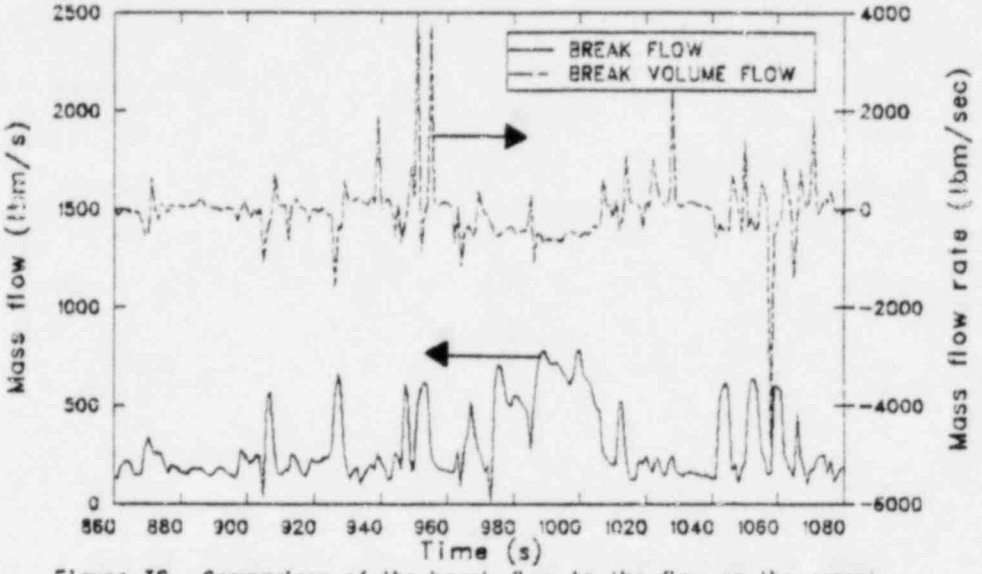

Figure 38. Comparison of the break flow to the flow on the vessel side of the break volume from the RELAP5 calculation (860 to 1080 s).

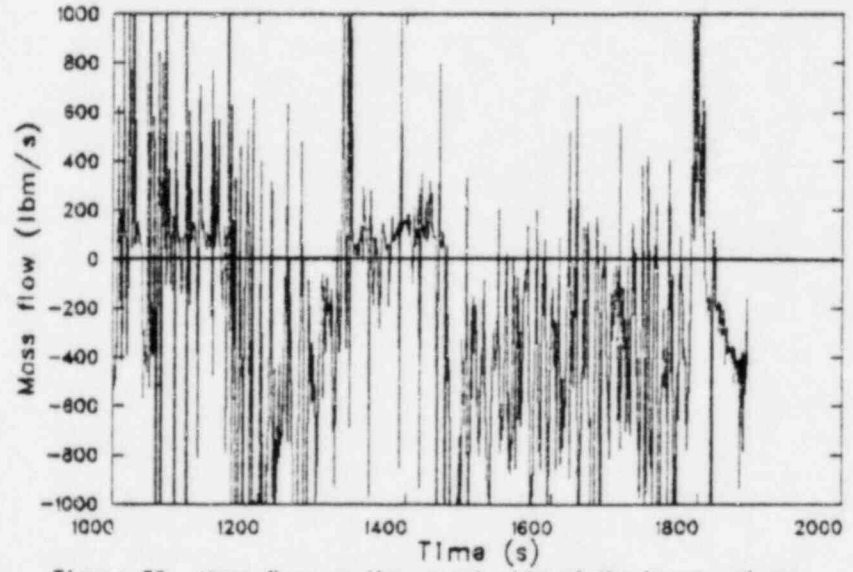

Figure 39. Mass flow on the vessel side of the break volume from the RELAP5 calculation (1000 to 1900 s).

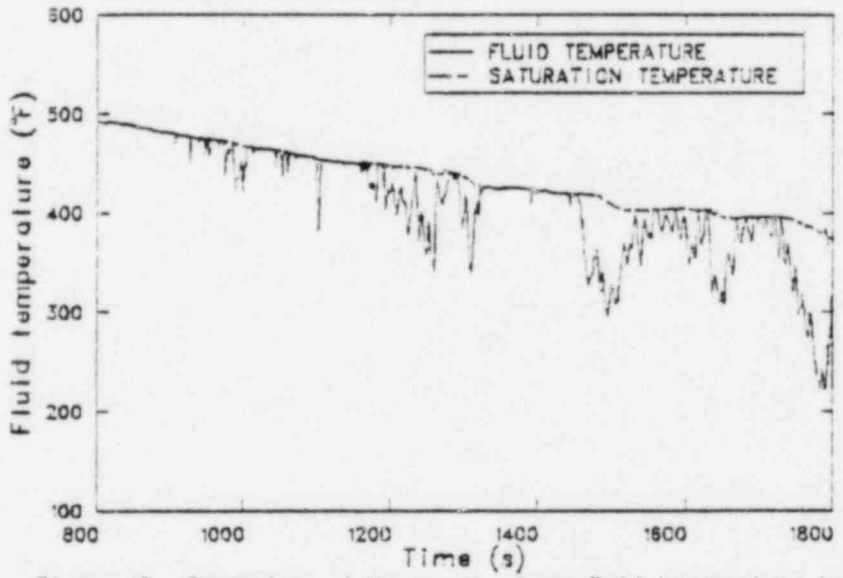

Figure 40. Comparison of the break volume fluid temperature to the corresponding saturation temperature from the RELAP5 calculation (800 to 1800 s).

injection rates and core decay power) were not necessarily the same as those assumed for the RELAP5 calculation.

Based on the similarities in overall system response between the small break tests conducted in the LOFT and Semiscale systems (and in particular the three tests mentioned above), and the RELAP5 calculated system response, the RELAP5 results are considered to be representative of the system behavior that will occur in a small break LOCA. Generally, the system response in the experiments (including trends in data as well as particular phenomena which occurred during the transients) was similar to the response obtained in the RELAP5 calculation for the RESAR-3S plant. Voiding of the system progressed from the upper elevations downward with the gradual formation and then blowout of the loop seal. Depletion of liquid from the primary system via the break was not sufficient to cause a sustained uncovering of the core either prior to or following blowout of the loop seal, and no heatup of the fuel/heater rods was observed. The ECC injection rates from the accumulators were very low (because of the small differential pressure between the accumulators and primary system), and in some instances the accumlators exhibited an on/off behavior similar to that shown in the RELAP5 calculation. Differences in the timing of events which occurred in the experiments, relative to the timing of the same event in the RELAP5 calculation, do occur. However, these differences in timing are attributable to scaling influences, as well as to the differences in boundary conditions assumed for the individual tests. The particular effect of cold ECC fluid on increasing the break flow rate (as occurs in the RELAP5 calculation) was not readily evident in the experiments. However, the ECC injection locations in the experiments were located well away from the break location (as compared to at the break in the RELAP5 calculation), and the injection rates were considerably less than that assumed for the RELAP5 calculation. Both of these factors would tend to reduce the amount of fluid subcooling at the break, thus reducing the magnitude of any possible increase in break flow that may occur.

6.2 RELAP5/Westinghouse Calculation Comparisons

In this section, comparisons of results from the RELAP5 small break calculation and from a Westinghouse evaluation model calculation for a

RESAR-3S plant are presented. These comparisons quantify conservatisms in the Westinghouse analysis required by 10 CFR 50.46 and Appendix K to 10 CFR 50.

The assumptions used in the RELAP5 best estimate calculation and in the Westinghouse evaluation model calculation are discussed in Section 4 of this report. The assumptions which provide the most significant degree of conservatism in the Westinghouse EM calculation relative to the RELAP5 calculation are as follows. First, the EM calculation assumes a significantly reduced ECC injection capability, both with respect to injection rates, and with respect to ECC fluid conditions. Second, the EM calculation assumes a high core decay power. The net effect of the first assumption is to reduce the likelihood that the core will remain covered during the transient (and, as shown below, the core is uncovered for a period of about 500 seconds in the EM calculation). The net effects of the second assumption are to cause a higher rate of conversion of core coolant to steam (thus maintaining a higher transient system pressure, as well as assuring a faster depletion of the available primary system liquid inventory), and to increase the rate of fuel rod heatup and the magnitude of the peak cladding temperatures once the core becomes uncovered. Other assumptions listed in Table 1 of Section 4 add to the conservative nature of the Westinghouse calculation, but to a lesser degree. The comparisons presented in the remaining paragraphs of this section illustrate the conservative nature of the Westinghouse calculation, especially with respect to peak cladding temperatures obtained during the transient.

The primary system pressure response (pressurizer pressure) for the RELAP5 and Westinghouse calculations is compared in Figure 41. The considerably faster overall depressurization in the RELAP5 calculation is attributed to the lower core transient decay power (see Figure 3), as well as to the higher ECC injection relative to the Westinghouse calculation. These two factors, when combined, result in a generally more rapid cooling of the primary system fluid in the RELAP5 calculation, along with a corresponding faster reduction of the primary system pressure (saturation

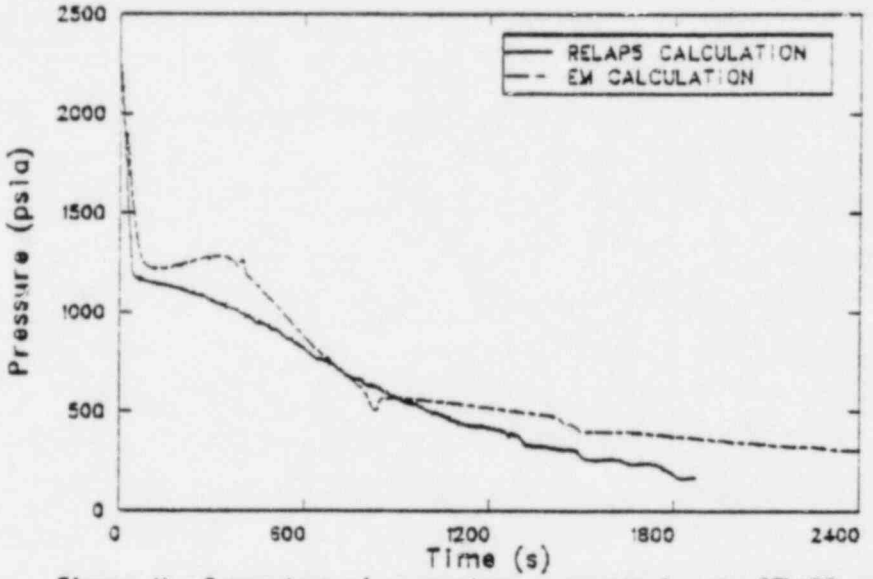

Figure 41. Comparison of pressurizer pressures for the RELAP5 and EM calculations.

pressure). (Figure 42 compares the total transient ECC mass[a] injected into the system for both calculations, and illustrate the much greater amount injected for the RELAP5 transient.) Although the primary system depressurizes to the accumulator setpoint pressure by about 800 seconds in the Westinghouse calculation (as compared to 858 seconds in the RELAP5 calculation), depressurization continues at a considerably faster rate in the RELAP5 calculation after this point. Thus, RHR pumped injection begins by 1760 seconds in the RELAP5 calculation, whereas the RHR setpoint pressure is not reached by the termination of the Westinghouse calculation at about 2500 seconds (although primary system mass inventory is increasing without RHR pumped injection).

The break flow rates for the RELAP5 and Westinghouse calculations are compared in Figure 43. The difference in flow rates up to about 200 seconds is due to the difference in transient system pressure (Figure 41), with the higher break flow rate in the EM calculation corresponding to the higher transient system pressure during this period. The increase in break flow at about 200 seconds in the RELAP5 calculation (as discussed in Section 6.1.4) is a result of the increase in subcooling in the break volume due to the reversal of flow in the broken loop cold leg. However, the increase in break flow in the Westinghouse calculation beginning at about 150 seconds is a result of increasing system pressure. Both calculations show a rapid reduction in break flow as blowout of the loop seal (at 400 seconds in the Westinghouse calculation and 520 seconds in the RELAP5 calculation) clears liquid from the break region. The high break flow in the RELAP5 calculation after accumulator injection begins is again a result of the increased subcooling in the break volume. The Westinghouse calculation does not show a corresponding increase in break flow rate when accumulator flow begins because the broken loop accumulator is assumed to discharge directly to containment without interacting with primary system fluid.

---

a. ECC flow rates from all active components are first added, then integrated, to obtain the results presented in the figure.

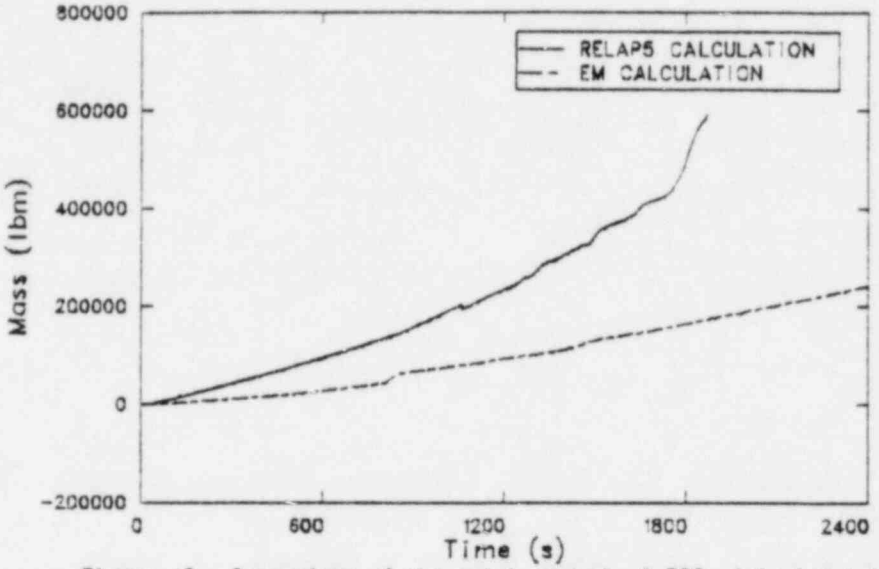

Figure 42. Comparison of the total amount of ECC injected into the primary system for the RELAP5 and EM calculations.

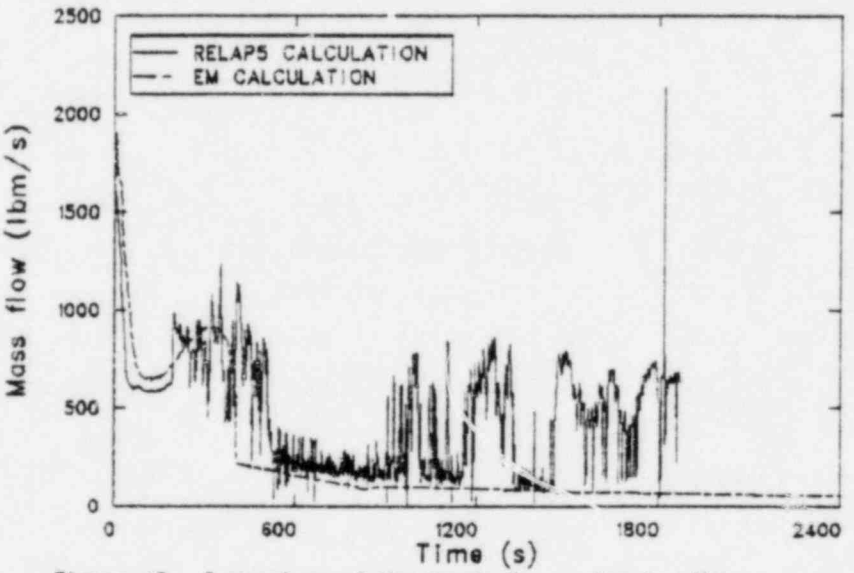

Figure 43. Comparison of the break flow rates for the RELAP5 and EM calculations.

The primary system transient mass inventories for the two calculations are compared in Figure 44. Considerably faster mass depletion occurs in the Westinghouse calculation following rupture because of the higher break flow rate and because of the lower ECC injection rates. The magnitude of the system mass inventory between about 340 and 850 seconds is sufficiently low in the Westinghouse calculation that the core becomes uncovered (see below), and a temperature excursion in the upper half of the core occurs. The temperature excursion is terminated once accumulator injection begins, as the gradual increase in the primary system mass inventory causes the vessel mixture level to rise above the top of the core. In the RELAP5 calculation, the system mass inventory remains well above that in the Westinghouse calculation until after accumulator injection begins, and as discussed earlier the core uncovers only briefly during this period (i.e., just prior to loop seal blowout). The primary system mass inventory in the RELAP5 calculation drops below that in the Westinghouse calculation after accumulator injection begins as a result of the much higher break flow rate discussed above. However, because of differences in primary system mass distribution, only brief periods of uncovering of the core occur during the accumulator injection period in the RELAP5 calculation, even though the total primary system mass inventory is less than the minimum inventory that caused uncovering of the core in the Westinghouse calculation. Both calculations show an increasing primary system mass inventory prior to the termination of the transient.

Figure 45 compares the mixture level in the core for the two calculations. RELAP5 does not calculate a mixture level. The mixture level presented in the figure for the RELAP5 calculation is derived from core fuel pin temperatures. The heat structure representing the fuel pin is assumed to be uncovered when a temperature increase occurs, and is assumed to be covered when temperatures follow the volume fluid temperatures. Again, the mixture level in the RELAP5 calculation drops below the top of the core only briefly during the transient, and only the top third of the core is uncovered during these periods. However, the Westinghouse calculation shows a relatively prolonged period, starting at about 340 seconds, when the mixture level drops well below the top of the

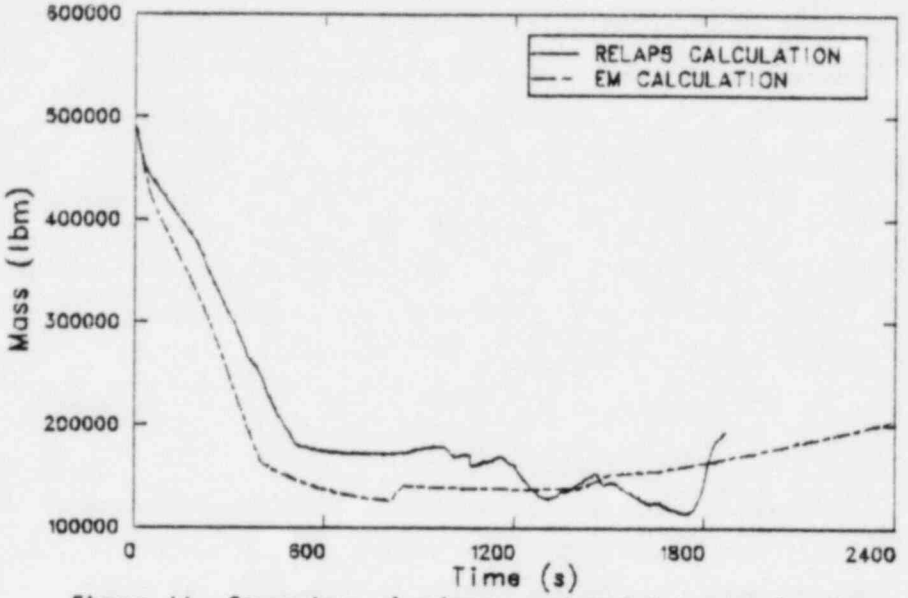

Figure 44. Comparison of primary system total mass for the RELAP5 and EM calculations.

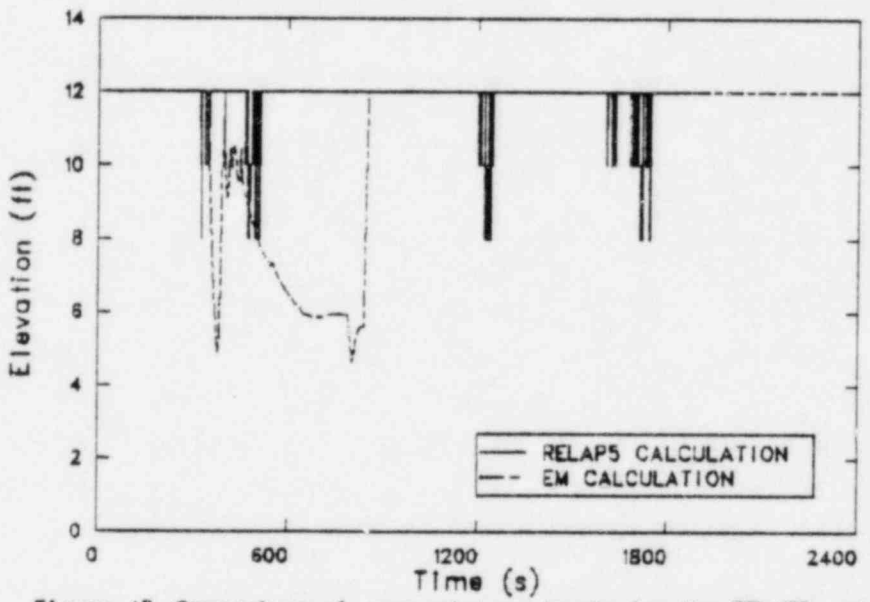

Figure 45. Comparison of core mixture levels for the RELAP5 and EM calculations.

core with the minimum mixture level being at about 5 ft above the bottom of the core. The mixture level remains below the top of the core until about 850 seconds when accumulator injection causes the rapid level increase shown in the figure. Figure 46 compares the cladding temperatures on the top 2 feet of the hot pin for the two calculations, and illustrates the differences in temperature response corresponding to the differences in core mixture levels. The peak cladding temperature in the EM calculation reaches about 1760°F, as compared to a peak cladding temperature in the RELAP5 calculation of considerably less than the full power steady state temperature of about 670°F. Figure 47 presents similar results to Figure 46, but for the 8 to 10 foot elevation above the bottom of the core. The hot pin heat transfer coefficients for the top 2 feet of the core are compared in Figure 48, and Figure 49 compares the hot spot fluid temperatures for the two calculations. The differences in response due to core mixture level differences are again evident.

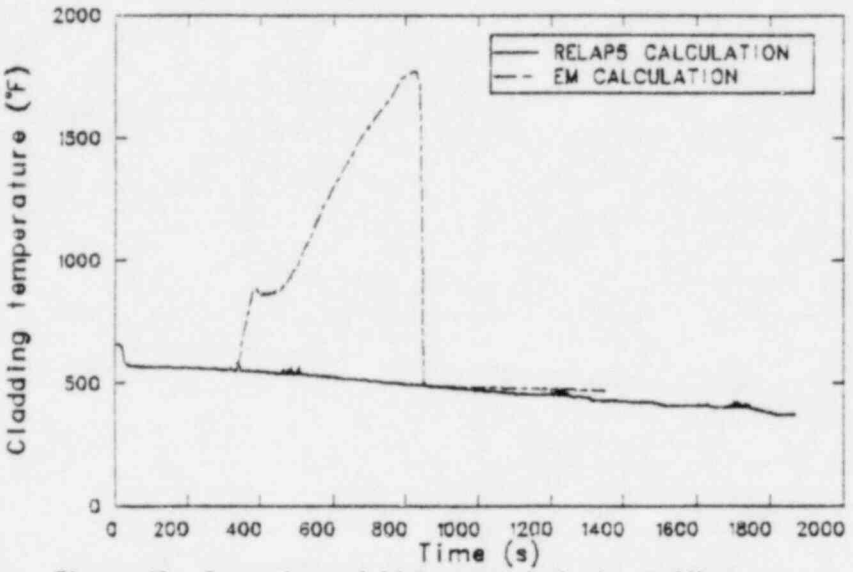

Figure 46. Comparison of high power fuel pin cladding temperatures for the RELAP5 and EM calculations at the 10 to 12 foot elevation.

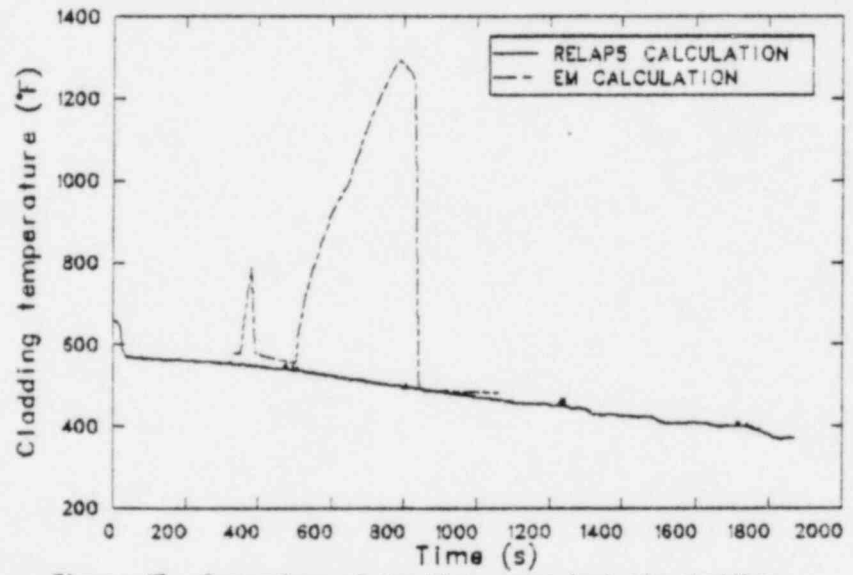

Figure 47. Comparison of the high power fuel pin cladding temperatures for the RELAP5 and EM calculations at the 8 to 10 foot elevation.

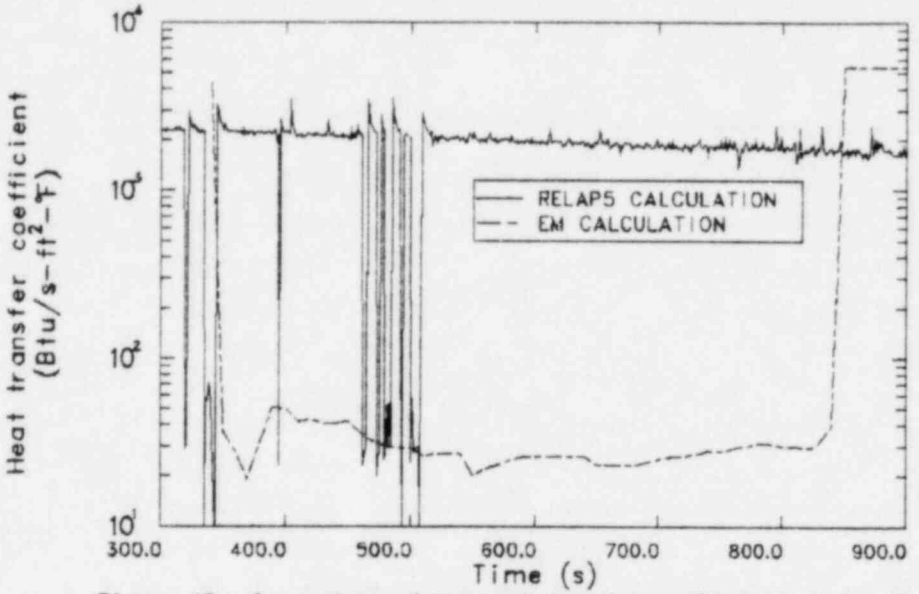

Figure 48. Comparison of the heat transfer coefficient at the 10 to 12 foot elevation on the high power fuel pin for the RELAP5 and EM calculations.

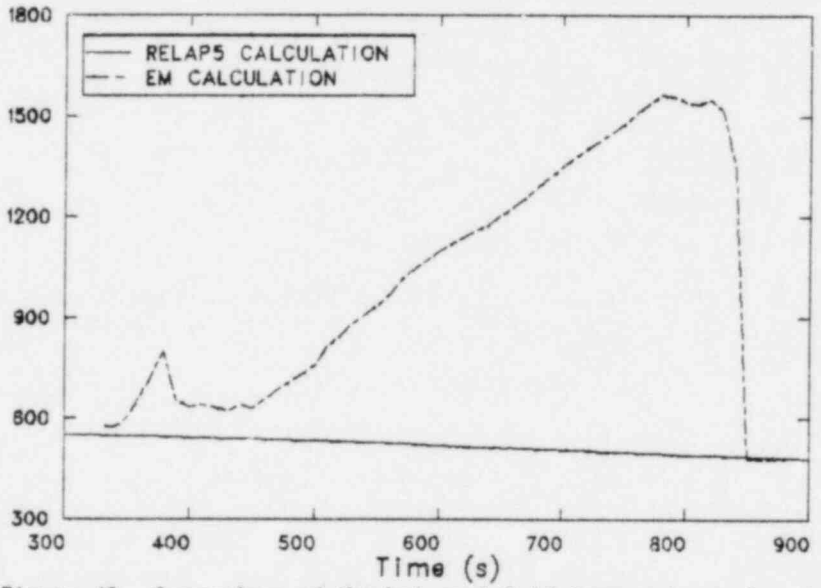

Figure 49. Comparison of the hot spot fluid temperatures for the RELAP5 and EM calculations.

7. CONCLUSIONS

The analysis of the RELAP5 results from the RESAR-3S small break calculation, and the comparison of the RELAP5 results with the results from a Westinghouse evaluation model calculation for a RESAR-3S plant have led to the following conclusions:

1. Based on the similarity of the RELAP5 results with available small break experimental data, the RELAP5 results are considered representative of the response expected for the limiting small break transient with "best estimate" assumptions.

   System response to the small break is characterized by a continuous primary side depressurization with only brief periods of dryout of the top third of the core. Maximum cladding temperature increases during the periods of dryout are limited to less than 30°F, and cladding temperatures remain less than the full power steady state temperatures throughout the transient.

2. The requirements for evaluation model small break calculation specified by 10 CFR 50.46 and Appendix K to 10 CFR 50 result in significant conservatisms in calculated system response relative to "best estimate" calculations.

   Comparisons of the EM and best estimate calculations show a considerably slower overall system depressurization rate in the EM calculation, and a prolonged period during which the top half of the core is uncovered. Peak cladding temperatures during the period of core dryout in the EM calculation reach about 1760°F, again as compared to peak cladding temperatures in the best estimate calculation of less than the initial temperature of about 670°F. The differences in system reponse between the two calculations are attributed primarily to the significantly reduced ECC injection capability and to the higher core decay power assumed in the EM calculation.

8. REFERENCES

1. V. H. Ranson et al., RELAP5/MOD1 Code Manual, NUREG/CR-1826, Idaho National Engineering Laboratory, November 1980.

2. Westinghouse Nuclear Energy Systems, Reference Safety Analysis Report, July 1975.

3. V. H. Ransom et al., "RELAP5 System Modeling Capability for Small Break LOCA," ANS Specialists Meeting on Small Break Loss-of-Coolant Accident Analyses in LWRs, Monterey, California, August 25-27, 1981, pp. 3-13 to 3-25.

4. H. S. Ozmelek and D. A. Driscoll,"Comparison of RELAP5 and RELAP4 LOFT Small Break Experimental Safety Analysis Models," ANS Specialists Meeting on Small Break Loss-of-Coolant Accident Analyses in LWRs, Monterey, California, August 25-27, 1981, pp. 3-135 to 3-166.

5. H. H. Kuo, H. M. Chow, and V. H. Ransom, "RELAP5 Horizontal Stratified Flow Model with Application to a Wyle LOFT Nozzle Calibration Experiment," ANS Specialists Meeting on Small Break Loss-of-Coolant Accident Analyses in LWRs, Monterey, California, August 25-27, 1981, pp. 6-91 to 6-110.

6. C. B. Davis, S. M. Modro, and T. H. Chen, "RELAP5 Calculations of the Effect of Primary Coolant Pump Operation During LOFT and Semiscale Small Break Experiments," ANS Specialists Meeting on Small Break Loss-of-Coolant Accident Analyses in LWRs, Monterey, California, August 25-27, 1981, pp. 6-111 to 6-127.

7. M. T. Leonard, Posttest RELAP5 Simulations of the Semiscale S-UT Series Experiment, Idaho National Engineering Laboratory, October 1981.

8. L. T. L. Dad and J. M. Carpenter, Experiment Data Report for LOFT Nuclear Small Break Experiment L3-5/L3-5A, NUREG/CR-1695, EG&G Idaho, Inc. November 1980.

9. J. M. Cozzuol, Quick Look Report for Semiscale Mod-3 Small Break Test S-SB-2, EGG-SEMI-5073, EG&G Idaho, Inc., December 1979.

10. D. J. Shimeck, J. E. Blakely, B. W. Murri, Quick Look Report for Semiscale Mod-2A Test S-UT-4 EGG-SEMI-5429, EG&G Idaho, Inc. April 1981.

APPENDIX A
RELAP5 UPDATES

APPENDIX A
RELAP5 UPDATES

Table A-1 contains the updates to RELAP5/MOD1 that were used up to 1522 s. Table A-2 contains the updates used from 1522 s to the end of the calculation. Comments in the update files explain the purpose of each update.

TABLE A-1. RELAP5 UPDATES USED FROM 0 TO 1522 S.

```
*COMPILE DEFINE,SEGUIR
*/
*/ DONORS VELOCITY TERM IN MOMENTUM FLUX EQUATION
*/
*IDENT BRFIX
*DELETE,VEXPLT.142,VEXPLT.143
      CONVF=CONVF+ABS(VELF(L))*DIFVF(L4)*SCRACH*ARAT(I+1)**2
      CONVG=CONVG+ABS(VELG(L))*DIFVG(L4)*SCRACH*ARAT(I+1)**2
*DELETE,VEXPLT.148,VEXPLT.149
      CONVF=CONVF-ABS(VELF(K))*DIFVF(K4)*SCRACH*ARAT(I)**2
      CONVG=CONVG-ABS(VELG(K))*DIFVG(K4)*SCRACH*ARAT(I)**2
*/
*IDENT RJWR017
*/
*/  ADD MASS ERROR AND TOTAL MASS TO SCAN REQUEST VARIABLES.
*D VREQS.4
      INTEGER T1(4),T2(20),T3(10),T4(5),T5(5),T6(4),T7
*D VREQD.4
      DATA T1/*TIME*,*CPUTIME*,*EMASS*,*TMASS*/
*D SCNREQ.76
   15 DO 20 I = 1,4
*D SCNREQ.80,82
   21 IF (ITYPI .LT. 0) GO TO 19
      GO TO (24,22,25,26), I
   19 GO TO (501,501,17,17), I
   24 PCKCOD = SHIFT(.NOT.MASK(42).AND.(LOCF(TIMEHY)-LOCF(FA(0))),18)
*I SCNREQ.90
   25 PCKCOD = SHIFT(.NOT.MASK(42).AND.(LOCF(EMASS)-LOCF(FA(0))),18)
      GO TO 16
   26 PCKCOD = SHIFT(.NOT.MASK(42).AND.(LOCF(TMASS)-LOCF(FA(0))),18)
   16 IF (ITYP .EQ. 0) GO TO 1000
   17 CONV = CONMF
      LABL(1) = T1(I)
      LABL(3) = UNMS(L)
      GO TO 900
*D SCNREQ.42
      INTEGER UNHT(4),UNHC(4),UNMS(2)
*I SCNREQ.54
      DATA UNMS/*(KG)*,*(LB)*/
*D WRPLID.61,66
      J = J + 1
      K = K + 1
      DO 26 I = 1,4
        IBUF(J) = T1(I)
        IBUF(K) = 0
        J = J + 1
        K = K + 1
   26 CONTINUE
*D PLTWRT.29
      LFA(J+3) = EMASS
      LFA(J+4) = TMASS
      J = J + 5
*/
*/ ENSURES THAT ALL RESTART VARIABLES ARE DEFINED
*/
*D RJWR009.33,58
*/
*/ DONORS MASS TERMS IN MOMENTUM FLUX EQUATION
*/
*D RARR017.2,3
  130 CONVF = CONVF*RFVFJ
      CONVG=CONVG*RGVGJ
```

TABLE A-2. RELAP5 UPDATES USED FROM 1522 S TO END OF CALCULATION.

```
*COMPILE DEFINE,SEGDIR
*/
*/ DONORS VELOCITY TERM IN MOMENTUM FLUX EQUATION
*/
*IDENT BRFIX
*DELETE,VEXPLT.142,VEXPLT.143
      CONVF=CONVF+ABS(VELF(L))*DIFVF(L4)*SCRACH*ARAT(I+1)**2
      CONVG=CONVG+ABS(VELG(L))*DIFVG(L4)*SCRACH*ARAT(I+1)**2
*DELETE,VEXPLT.148,VEXPLT.147
      CONVF=CONVF-ABS(VELF(K))*DIFVF(K4)*SCRACH*ARAT(I)**2
      CONVG=CONVG-ABS(VELG(K))*DIFVG(K4)*SCRACH*ARAT(I)**2
*/
*/ MAKES ALL RESTART VARIABLES DEFINED
*D RJWROC9.33,58
*/
*/ DONORS MASS TERMS IN MOMENTUM FLUX EQUATION
*D RARR017.2,3
  13C   CONVF = CONVF*RFVFJ
      CONVG=CONVG*RGVGJ
*/
*/ DMK MASS ERROR FIXES
*IDENT DMKR018
*/
*/  ADD MASS ERROR AND TOTAL MASS TO SCAN REQUEST VARIABLES.
*D VREQS.4
      INTEGER T1(4),T2(20),T3(10),T4(5),T5(5),T6(4),T7
*D VREQD.4
      DATA T1/"TIME","CPUTIME","EMASS","TMASS"/
*D SCNREQ.76
   15   DO 20 I = 1,4
*D SCNREQ.80,82
   21   IF (ITYP(I .LT. 0) GO TO 19
      GO TO (24,22,25,25), I
   19   GO TO (501,501,17,17), I
   24   PCKCOD = SHIFT(.NOT.MASK(42).AND.(LOCF(TIMEHY)-LOCF(FA(0))),18)
*I SCNREQ.90
   25   PCKCOD = SHIFT(.NOT.MASK(42).AND.(LOCF(EMASS)-LOCF(FA(0))),18)
      GO TO 16
   26   PCKCOD = SHIFT(.NOT.MASK(42).AND.(LOCF(TMASS)-LOCF(FA(0))),18)
   16   IF (ITYP .EQ. 0) GO TO 1000
   17   CONV = CONVF
      LABL(1) = T1(I)
      LABL(3) = UNMS(L)
      GO TO 900
*D SCNREQ.42
      INTEGER UNHT(4),UNHC(4),UNMS(2)
*I SCNREQ.54
      DATA UNMS/"(KG)","(LB)"/
*D WRPLIC.61,66
      J = J + 1
      K = K + 1
      DO 26 I = 1,4
        IBUF(J) = T1(I)
        IBUF(K) = 0
        J = J + 1
        K = K + 1
   26   CONTINUE
*D PLTWRT.29
      LFA(J+3) = EMASS
      LFA(J+4) = TMASS
      J = J + 5
*/    MASS ERROR IN STATE
*D HXCROC8.2199,HXCR010.8
C
C ... DEBUG PRINT OF MASS ERROR
C
      IF (HELP .NE. 0)
     * WRITE (OUTPUT, 8001) TIMEHY, DT, NCOUNT, HELP, SUCCES, FAIL
```

TABLE A-2. (continued)

```
      TMASS       =  0.0
      TDEMAS      =  0.0
      ERRMMX      = -1.0
      DEMAXS      =  0.0
      SUMASS      =  0.0
      GLOBAL      =  0.0
      JVOLS       =  0
      ITER        =  0
      JTER        =  0
C
      DO 1500 I = IV, IVE, IVSKP
      IF (VCTRL(I) .LT. 0) GO TO 1500
      ERRHO       = RHO(I) - RHOM(I)
      DEMASS      = V(I) * ERRHO
      DTMASS      = V(I) * RHO(I)
C
      TDEMAS      = TDEMAS + DEMASS
      TMASS       = TMASS + DTMASS
      GLOBAL      = GLOBAL + DEMASS * DEMASS
      SUMASS      = SUMASS + DTMASS * DTMASS
      JVOLS       = JVOLS + 1
C
      ERRM        = ERRHO / RHOF(I)
C
      ERRMX       = ERRHO / RHO(I)
C
      IF (ABS(ERRM) .LT. 2.0E-3) GO TO 1501
      VCTRL(I)    = VCTRL(I) .OR. SHIFT(MASK(1), 10)
 1501 IF (ABS(ERRM) .LE. ERRMMX) GO TO 1502
      ITER        = I
      ERRMMX      = ABS(ERRM)
 1502 IF (ABS(DEMASS) .LE. DEMAXS) GO TO 1505
      JTER        = I
      DEMAXS      = ABS(DEMASS)
 1505 IF (HELP .NE. 0)
     *WRITE (OUTPUT, 8010) I, VOLNO(I), V(I), RHO(I), RHOM(I), ERRM,
     *                     ERRMX, DEMASS
 1500 CONTINUE
C
      EMASS       = EMASS + TDEMAS
      RMSVRO      = SQRT(SUMASS / FLOAT(JVOLS))
      SUMASS      = 1.0 / SUMASS
      SCALER      = SQRT(3.8416 * FLOAT(JVOLS) / AMAX0(1, (JVOLS - 1)))
      VERRMX      = DEMAXS / RMSVRO
      RMSERR      = SQRT(GLOBAL * SUMASS)
      GLOBAL      = SCALER * RMSERR
      IF (VERRMX .LE. ERRMMX) GO TO 1510
      IF (JTER .NE. 0) VCTRL(JTER) = VCTRL(JTER) .OR. SHIFT(MASK(1), 13)
      GO TO 1511
 1510 IF (ITER .NE. 0) VCTRL(ITER) = VCTRL(ITER) .OR. SHIFT(MASK(1), 13)
 1511 ERRMAX      = AMAX1(ERRMMX, VERRMX, GLOBAL)
      IF (ERRMAX .GE. 2.0E-3) SUCCES = 1
C
       IF (HELP .NE. 0)
     * WRITE (OUTPUT, 8030) TDEMAS, TMASS, EMASS, ERRMMX, VOLNO(ITER),
     *                      VERRMX, VOLNO(JTER), GLOBAL, RMSVRO,
     *                      RMSERR, SUCCES, ERRMAX
C
*D HXCR008.2216
 1600 IF (HELP .EQ. 0) GO TO 1650
      WRITE (OUTPUT,8001) TIMEHY, DT, NCOUNT, HELP, SUCCES, FAIL
      IF (CHECK .EQ. 0) WRITE (OUTPUT,8002) CHECK
      IF (CHECK .EQ. 1) WRITE (OUTPUT,8003) CHECK
      CALL STRACE
      CALL HELPTR("STATE")
*I HXCR008.2217
C
C *** FORMATS
```

TABLE A-2. (continued)

```
*D JPROP.89
  900    CONTINUE
         VOIDS          = VOIDFJ(I) + VOIDGJ(I)
         IF (HELP .EQ. 0) GO TO 12
         VOIDSK         = VOIDF(K) + VOIDG(K)
         WRITE (OUTPUT,9022) "KVOL", VOIDF(K), RHOF(K), UF(K),
        *                            VOIDG(K), RHOG(K), UG(K),
        *                            CCAK, VOIDSK
         VOIDSL         = VOIDF(L) + VOIDG(L)
         WRITE (OUTPUT,9022) "LVOL", VOIDF(L), RHOF(L), UF(L),
        *                            VOIDG(L), RHOG(L), UG(L),
        *                            CCAL, VOIDSL
         VF             = VELFJ(I)
         VG             = VELGJ(I)
         WRITE (OUTPUT, 9021) "JNEW", VF, VOIDFJ(I), RHOFJ(I), JFJ(I),
        *                            VG, VOIDGJ(I), RHOGJ(I), JGJ(I),
        *                            CCAJ(I), VOIDS
   12    CONTINUE
         IF ((VELGJ(I) * VELFJ(I)) .LE. 0.0) GO TO 848
*I JPROP.114
         IF (HELP .EQ. 0) GO TO 900
         VOIDS          = VOIDFJ(I) + VOIDGJ(I)
         WRITE (OUTPUT, 9023) "STR", VOIDFJ(I), VOIDGJ(I), VOIDS
*D JPROP.119
         IF (VOIDS .LE. 1.0) GO TO 900
*D JPROP.122,175
         IF (HELP .NE. 0) WRITE (OUTPUT,9023) "NORM", VOIDFJ(I),
        *                                             VOIDGJ(I), VOIDS
*I JPROP.177
C
C *** DEBUG FORMATS
C
 9000 FORMAT("0", 134("*"),/," JPROP DIAGNOSTIC PRINTOUT, TIMEHY =",
     *1PG15.7,", DT =",1PG15.7,", NCOUNT =",I10,", HELP =",I3,
     *", SUCCES =",I3,", FAIL =",L2)
 9010 FORMAT("0JUNCTION DONORED PROPERTIES, ICHOKE =",I3,", KBAD =",I10,
     *//," ",134("="),/,
     *" ",2X,"I",4X,"JUNNO(I)",8X,"K",8X,"VOLNO(K)",9X,"L",8X,"VOLNO(L)"
     *,/,
     *" ",6X,"VELFJ - VELJ",4X,"VOIDFJ",7X,"RHOFJ",9X,"UFJ",6X,
     *"VELGJ - VELJ",4X,"VOIDGJ",7X,"RHOGJ",9X,"UGJ",10X,"CCAJ",8X,
     *"VOIDS",/," ",134("="))
 9020 FORMAT(A1,I6,I11,I10,I15,I11,I15)
 9021 FORMAT(" ",A5,1P10G13.5)
 9022 FORMAT(" ",A5,13X,1P3G13.5,13X,1P5G13.5)
 9023 FORMAT(" ",A5,13X,1P1G13.5,2(39X,1P1G13.5))
 9030 FORMAT(" CHOKED...SKIP JUNCTION DONORING")
*/    UPDATES TO REDO PRESEQ...VFINL AND/OR CUT THE TIME STEP AND REPEAT
*/    (SUCCES = 3) IF VELOCITIES FLIP-FLOP. (SUBROUTINES SYSSOL, VFINL,
*/    DTSTEP, HYDRO, TRAN)
*D SYSSOL.80
         P(I)           = PO(I) + SOURCP(J)
*D VFINL.2
      SUBROUTINE VFINL(ICYCLE, JREDO)
*I VFINL.11
      REAL VELFJX(1), VELGJX(1)
      EQUIVALENCE (VELFJX(1), VELJ(1)), (VELGJX(1), VELJO(1))
      REAL ERRHO(1)
      EQUIVALENCE (ERRHJ(1), VNEW(1))
      LOGICAL ICYCLE
*I VFINL.12
C     INITIALIZE MASS ERROR = 0.0
      ICYCLE        = .FALSE.
      DO 20 I = IV, IVE, IVSKP
         ERRHO(I)   = 0.0
   20 CONTINUE
      IF (JREDO .GT. 1) GO TO 30
```

TABLE A-2. (continued)

```
*D RJWR009.62
          IF ( VOIDS .LE. 1.0 )  GO TO  899
*D RJWR009.65,115
*/    JPROP...DO NUMERICAL AVERAGE OF JUNCTION PROPERTIES AT J VELOCITY,
*/             INCLUDE REDOND' LOGIC FOR VELOCITY FLIP-FLOP ( ICHOKE = 2,
*/             MODIFIES IMREG...JUN DATA BLOCK) AND DELETE PUNT LOGIC FOR
*/             VOIDFJ + VOIDGJ = 0.0.
*I JPROP.11
      REAL VELFJX(1), VELGJX(1)
      EQUIVALENCE (VELFJX(1), VELJ(1)), (VELGJX(1), VELJO(1))
C
      INTEGER OUTPUT
      DATA OUTPUT/6LOUTPUT/
C
      LINCTL      = " "
      IF (HELP .EQ. 0) GO TO 10
      WRITE (OUTPUT, 9000) TIMEHY, DT, NCOUNT, HELP, SUCCES, FAIL
      CALL STRACE
      WRITE (OUTPUT, 9010)ICHOKE
   10 CONTINUE
C
*D JPROP.15,16
*I JPROP.21
         INAME        = "JOLD"
         VF           = VELFJO(I)
         VG           = VELGJO(I)
         VOIDS        = VOIDFJ(I) + VOIDGJ(I)
         IF (ICHOKE .EQ. 0) GO TO 1
         IF (ICHOKE .EQ. 1) GO TO 2
         INAME        = "JEXP"
         VF           = VELFJX(I)
         VG           = VELGJX(I)
         IF (SHIFT(IMREG(I), 43) .GE. 0) GO TO 900
         IF ((IJ2(I) .LT. 0) .AND.
     *       (SHIFT(JC(I+1), 4) .LT. 0)) INAME = "SKIP"
         GO TO 1
      2  IF ((IJ2(I) .LT. 0) .AND.
     *       (SHIFT(JC(I+1), 4) .LT. 0)) INAME = "SKIP"
      1  IF (HELP .EQ. 0) GO TO 3
         WRITE (OUTPUT, 9020) LINCTL, I, JUNNO(I), K,
     *                        VOLNO(K), L, VOLNO(L)
         LINCTL       = "0"
         WRITE (OUTPUT, 9021) INAME, VF, VOIDFJ(I), RHOFJ(I), UFJ(I),
     *                                VG, VOIDGJ(I), RHOGJ(I), UGJ(I),
     *                                CCAJ(I), VOIDS
      3  IF (INAME .EQ. "SKIP") GO TO 900
*D JPROP.26
         IF (VELFJ(I)) 100, 200, 300
*D JPROP.33,42
*D JPROP.44
         VOIDFJ(I)    = 0.5 * (VOIDF(K) * RHOF(K) + VOIDF(L) * RHOF(L))
         UFJ(I)       = 0.5 * (AMAX1(1.0E-15, VOIDF(K)) * RHOF(K) * UF(K)
     *                       +  AMAX1(1.0E-15, VOIDF(L)) * RHOF(L) * UF(L))
         VOIDFJ(I)    = VOIDFJ(I) / RHOFJ(I)
         UFJ(I)       = UFJ(I) / (RHOFJ(I) * AMAX1(1.0E-15, VOIDFJ(I)))
*D JPROP.58
         IF (VELGJ(I)) 500, 600, 700
*D JPROP.66,77
*D JPROP.79,80
         VOIDGJ(I)    = 0.5 * (VOIDG(K) * RHOG(K) + VOIDG(L) * RHOG(L))
         UGJ(I)       = 0.5 * (AMAX1(1.0E-15, VOIDG(K)) * RHOG(K) * UG(K)
     *                       +  AMAX1(1.0E-15, VOIDG(L)) * RHOG(L) * UG(L))
         CCAJ(I)      = 0.5 * (AMAX1(1.0E-15, VOIDG(K)) * RHOG(K) * CCAK
     *                       +  AMAX1(1.0E-15, VOIDG(L)) * RHOG(L) * CCAL)
         VOIDGJ(I)    = VOIDGJ(I) / RHOGJ(I)
         RRHOGJ       = 1.0 / (RHOGJ(I) * AMAX1(1.0E-15, VOIDGJ(I)))
         UGJ(I)       = UGJ(I) * RRHOGJ
         CCAJ(I)      = CCAJ(I) * RRHOGJ
```

TABLE A-2. (continued)

```
C
 8001  FORMAT("0",134("*"),/," MASS ERROR DIAGNOSTIC PRINTOUT, TIMEHY ="
     * ,1P1G15.7,", DT =",1P1G15.7,", NCOUNT =",I10,", HELP =",I3,
     * ", SUCCES =",I3,", FAIL =",L2,/,"0",102("*"),/," I=",5X,"VOLNO",
     * 8X,"V",11X,"RHO",10X,"RHOM",5X,"DRHO / RHOF",3X,"DRHO / RHO",4X,
     * "V * DRHO",/,
     * " ",102("*"))
C
 8002 FORMAT(" STATE...RESET TO OLD TIME PROPERTIES, ( CHECK =",I3," )")
C
 8003 FORMAT(" STATE...FINAL SOLUTION PROPERTIES, ( CHECK =",I3," )")
C
 8010  FORMAT(" ",I6,I10,1P6G13.5)
C
 8030  FORMAT(" ",102("="),/,2X,"TOTAL DEMASS",68("_"),1P1G13.5,/,
     * "0     SYSTEM TOTAL MASS (TMASS) =",1P1G13.5,/,
     * "  CUMULATIVE MASS ERROR (EMASS) =",1P1G13.5,/,
     *                 MAXIMUM DRHO / RHOF =",1P1G13.5,
     * " ( VOLNO =",I10," )",/,
     *   MAXIMUM V * DRHO / RMS(MASS) =",1P1G13.5,
     * " ( VOLNO =",I10," )",/,
     * " GLOBAL ERROR (0.95 CONFIDENCE) =",1P1G13.5,
     * " ( RMS(MASS) =",1P1G13.5," GLOBAL RMS(ERROR) =",1P1G13.5," )",/,
     * 25X,"SUCCES =",I3,11X,"( ERRMAX =",1P1G13.5," )",/,
     * " ",102("="))
C
*/    UPDATES TO REMOVE ENERGY CORRECTION WHEN QUALS, QUALA TRUNCATED
*D HXCR008.32
          QUALA(I)    = QUALA0(I) + DELXA
*D HXCR008.42,71
C
C  ..... TEST FOR QUALS, QUALA TRUNCATION (KEEP U(I) SOLUTION)
C
          IF (((QUALS(I) .GT. -0.0005) .AND. (QUALS(I) .LT. 1.01)) .AND.
     *       ((QUALA(I) .GT. -0.0005) .AND. (QUALA(I) .LT. 1.01)) .AND.
     *       ((QUALA(I) - QUALS(I)) .LT. 0.0010) .AND.
     *       (RHOM(I) .GT. 0.0)) GO TO 201
          VCTRL(I)    = VCTRL(I) .OR. SHIFT(MASK(1), 12)
          SUCCES      = 1
  201     QUALCX      = 0.5 * AMAX1(0.0, (QUALA(I) - QUALS(I)))
          QUALA(I)    = AMIN1(1.0, AMAX1(0.0, (QUALA(I) - QUALCX)))
          QUALS(I)    = AMIN1(1.0, AMAX1(0.0, (QUALS(I) + QUALCX)))
          DOTM(I)     = DOTM(I)
     *                + DMDA(I) * ((QUALA(I) - QUALA0(I)) + DELXA)
     *                + DMDX(I) * (QUALS(I) - QUALS0(I))
*/    IJPROP...DO NUMERICAL AVERAGE OF JUNCTION PROPERTIES AT 0 VELOCITY
*D IJPROP.26
          IF (VELFJ(I)) 100,200,300
*D IJPROP.31,41
  200     CONTINUE
          RHOFJ(I)    = 0.5 * (RHOF(K) + RHOF(L))
          VOIDFJ(I)   = 0.5 * (VOIDF(K) * RHOF(K) + VOIDF(L) * RHOF(L))
          UFJ(I)      = 0.5 * (AMAX1(1.0E-15, VOIDF(K)) * RHOF(K) * UF(K)
     *                +        AMAX1(1.0E-15, VOIDF(L)) * RHOF(L) * UF(L))
          VOIDFJ(I)   = VOIDFJ(I) / RHOFJ(I)
          UFJ(I)      = UFJ(I) / (RHOFJ(I) * AMAX1(1.0E-15, VOIDFJ(I)))
*D IJPROP.54,76
  600     CONTINUE
          RHOGJ(I)    = 0.5 * (RHOG(K) + RHOG(L))
          VOIDGJ(I)   = 0.5 * (VOIDG(K) * RHOG(K) + VOIDG(L) * RHOG(L))
          UGJ(I)      = 0.5 * (AMAX1(1.0E-15, VOIDG(K)) * RHOG(K) * UG(K)
     *                +        AMAX1(1.0E-15, VOIDG(L)) * RHOG(L) * UG(L))
          CCAJ(I)     = 0.5 * (AMAX1(1.0E-15, VOIDG(K)) * RHOG(K) * CCAK
     *                +        AMAX1(1.0E-15, VOIDG(L)) * RHOG(L) * CCAL)
          VOIDGJ(I)   = VOIDGJ(I) / RHOGJ(I)
          RRHOGJ      = 1.0 / (RHOGJ(I) * AMAX1(1.0E-15, VOIDGJ(I)))
          UGJ(I)      = UGJ(I) * RRHOGJ
          CCAJ(I)     = CCAJ(I) * RRHOGJ
```

TABLE A-2. (continued)

```
C  FIRST TIME THROUGH...SAVE EXPLICIT NEW TIME VELOCITIES
      DO 31 I = IJ, IJE, IJSKP
        VELFJX(I) = VELFJ(I)
        VELGJX(I) = VELGJ(I)
   31 CONTINUE
      GO TO 40
C  SECOND TIME THROUGH...INITIALIZE ERROR IN FLUX TERMS
   30 DO 32 I = IJ, IJE, IJSKP
        K = .NOT. MASK(43) .AND. SHIFT(IJ1(I), 18)
        IF (VCTRL(K) .GE. 0) ERRHO(K) = ERRHO(K) + MFLOWJ(I)
        K = .NOT. MASK(43) .AND. SHIFT(IJ2(I), 18)
        IF (VCTRL(K) .GE. 0) ERRHO(K) = ERRHO(K) - MFLOWJ(I)
   32 CONTINUE
*D VFINL.14
   40 J              = IXVF
*I VFINL.21
      IMREG(I)    = .NOT. SHIFT(MASK(1), 17) .AND. IMREG(I)
*I VFINL.37
      IF (JREDO .GT. 1) GO TO 130
C
C     FIRST TIME THROUGH
C
      IF ((VELFJX(I) * VELFJ(I) .LT. 0.0) .OR.
     *    ((VELFJX(I) .EQ. 0.0) .AND. (VELFJ(I) .NE. 0.0)) .OR.
     *    (VELGJX(I) * VELGJ(I) .LT. 0.0) .OR.
     *    ((VELGJX(I) .EQ. 0.0) .AND. (VELGJ(I) .NE. 0.0))) GO TO 131
      GO TO 140
  130 CONTINUE
C
C     SECOND TIME THROUGH
C
      IF ((VELFJX(I) * VELFJ(I) .GE. 0.)) .OR.
     *   (VELGJX(I) * VELGJ(I) .GE. 0.))) GO TO 140
  131 IMREG(I)    = SHIFT(MASK(1), 17) .OR. IMREG(I)
  140 ICYCLE      = ICYCLE .OR. (SHIFT(IMREG(I), 43) .LT. 0)
*D VFINL.40
C  REDONOR AND RESET FOR VELOCITY FLIPFLOP
      IF (.NOT. ICYCLE) GO TO 3010
      IF (JREDO .GT. 1) GO TO 3030
C  FIRST TIME THROUGH...REDONOR FLIPFLOP JUNCTIONS
      CALL JPROP(2)
C  ESTIMATE THE ERROR IN FLUX TERMS DUE TO FLIPFLOP
      DO 3001 I = IJ, IJE, IJSKP
        DMFLOW = AJUN(I) * (VOIDFJ(I) * RHOFJ(I) * VELFJ(I)
     *                    + VOIDGJ(I) * RHOGJ(I) * VELGJ(I))
     *         - MFLOWJ(I)
        K = .NOT. MASK(43) .AND. SHIFT(IJ1(I), 18)
        IF (VCTRL(K) .GE. 0) ERRHO(K) = ERRHO(K) - DMFLOW
        K = .NOT. MASK(43) .AND. SHIFT(IJ2(I), 18)
        IF (VCTRL(K) .GE. 0) ERRHO(K) = ERRHO(K) + DMFLOW
 3001 CONTINUE
C  RESET EXPLICIT VELOCITIES, SAVE FINAL VELOCITIES
      DO 3020 I = IJ, IJE, IJSKP
        SAVEF     = VELFJ(I)
        SAVEG     = VELGJ(I)
        VELFJ(I)  = VELFJX(I)
        VELGJ(I)  = VELGJX(I)
        VELFJX(I) = SAVEF
        VELGJX(I) = SAVEG
 3020 CONTINUE
      GO TO 3040
C  SECOND TIME THROUGH...ESTIMATE ERROR IN FLUX TERMS DUE TO FLIPFLOP
 3030 DO 3041 I = IJ, IJE, IJSKP
        K = .NOT. MASK(43) .AND. SHIFT(IJ1(I), 18)
        IF (VCTRL(K) .GE. 0) ERRHO(K) = ERRHO(K) - MFLOWJ(I)
        K = .NOT. MASK(43) .AND. SHIFT(IJ2(I), 18)
        IF (VCTRL(K) .GE. 0) ERRHO(K) = ERRHO(K) + MFLOWJ(I)
 3041 CONTINUE
C  ESTIMATE THE MASS ERROR
 3040 IMAXF  = 0
      EMAXF  = 0.0
      IMAXFG = 0
      EMAXFG = 0.0
      GLOBAL = 0.0
      SUMASS = 0.0
      JVOLS  = 0
```

TABLE A-2. (continued)

```
      DO 3031 I = IV, IVE, IVSKP
        IF (VCTRL(I) .LT. 0) GO TO 3031
        JVOLS     = JVOLS + 1
        DEMASS    = ABS(ERRHO(I)) * DT
        ERRHO(I)  = DEMASS / V(I)
        GLOBAL    = GLOBAL + DEMASS * DEMASS
        XMASS     = V(I) * RHO(I)
        SUMASS    = SUMASS + XMASS * XMASS
        ERRM      = ERRHO(I) / RHOF(I)
        IF (ERRM .LE. EMAXF) GO TO 3032
        IMAXF = I
        EMAXF = ERRM
 3032   IF (DEMASS .LE. EMAXFG) GO TO 3031
        IMAXFG = I
        EMAXFG = DEMASS
 3031 CONTINUE
      SUMASS = 1.0 / SUMASS
      SCALER = 3.8416 * FLOAT(JVOLS) / AMAX0(1, (JVOLS - 1))
      EMAXX  = AMAX1(EMAXF,
     *               EMAXFG * SQRT(FLOAT(JVOLS) * SUMASS),
     *               SQRT(SCALER * GLOBAL * SUMASS))
      IF (EMAXX .LT. 2.0E-3) ICYCLE = .FALSE.
      IF ((ICYCLE) .OR. (JREDO .GT. 1)) GO TO 3010
C  FIRST TIME THROUGH... SMALL ERROR, RESET DONORING, FINAL VELOCITIES
      CALL JPROP(2)
      DO 3011 I = IJ, IJE, IJSKP
        VELFJ(I) = VELFJX(I)
        VELGJ(I) = VELGJX(I)
 3011 CONTINUE
 3010 CONTINUE
*D DTSTEP.2
      SUBROUTINE DTSTEP(DTLIMT)
*D HYDRO.2
      SUBROUTINE HYDRO(DTLIMT,NREDO)
*I HYDRO.10
      LOGICAL ICYCLE
*I HYDRO.51
      JREDO     = 0
*I HYDRO.52
  100 CONTINUE
      JREDO     = JREDO + 1
*D HYDRO.71
      CALL VFINL(ICYCLE, JREDO)
      IF (.NOT. ICYCLE) GO TO 110
      IF (JREDO .EQ. 1) GO TO 100
      SUCCES    = 3
      IF (0.5 * DT .LT. DTLIMT) GO TO 110
      NREDO = NREDO + 1
      GO TO 1000
  110 CONTINUE
*I HYDRO.83
      IF (SUCCES .EQ. 3) SUCCES = 0
*I TRAN.12
      DATA  NREDO/ 0 /
C
*D TRAN.17
    5 CALL DTSTEP(DTLINT)
*D TRAN.44
   11 CALL HYDRO(DTLIMT,NREDO)
*I TRAN.60
      WRITE (OUTPUT,2005) NREDO
 2005 FORMAT ("0***** NUMBER OF TIME STEP REPEATS DUE TO VELOCITY FLIP-F
     *LOP ",I10)
*/    FIX MOVER TO RESET STATE IF SUCCES = 3
*D MOVER.17
*/    CORRECTIONS TO WALL FRICTION, FORM LOSS AND DISSIPATION IN VEXPLT
*D HXCRO13.11,15
        AVRF      = VOIDFA * RHOFA
        AVRG      = VOIDGA * RHOGA
```

TABLE A-2. (continued)

```
C
            RAVRF       = 1.0 / (RHOFA * AMAX1(1.0E-15, VOIDFA))
            RAVRG       = 1.0 / (RHOGA * AMAX1(1.0E-15, VOIDGA))
C
            RFVFJ       = 0.5 * VOIDFJ(I) * RHOFJ(I) * RAVRF
            RGVGJ       = 0.5 * VOIDGJ(I) * RHOGJ(I) * RAVRG
C
*D VEXPLT.131,132
C
C ----- LIQUID FRICTION
C
            FRICFK      = FWALF(K) * DXK * VOIDF(K) * RHOF(K) * RAVRF
C
            FRICFL      = FWALF(L) * DXL * VOIDF(L) * RHOF(L) * RAVRF
C
C ----- VAPOR FRICTION
C
            FRICGK      = FWALG(K) * DXK * VOIDG(K) * RHOG(K) * RAVRG
C
            FRICGL      = FWALG(L) * DXL * VOIDG(L) * RHOG(L) * RAVRG
C
C ----- JUNCTION FRICTION
C
            FRICFJ      = FRICFK + FRICFL
            FRICGJ      = FRICGK + FRICGL
*D HXCR013.25
            FJFG        = (FJFG + FIJ(I) * DX) * (RAVRG + RAVRF)
*D VEXPLT.215
*D HXCR013.32
*D VEXPLT.217
*D HXCR013.33
            VPGNX       = AMAX1(0.0, (VPGEN * RAVRG))
     *                  - AMIN1(0.0, (VPGEN * RAVRF))
*D VEXPLT.281,282
*D HXCR013.38,39
*D VEXPLT.286,291
*D HXCR013.40
*D VEXPLT.293
            HLSF        = HLOSSF * AVRF * AJDT * VELFJO(I)
            HLSG        = HLOSSG * AVRG * AJDT * VELGJO(I)
            DISPK       = HLSF * AMIN1(0.0, VELFJO(I))
     *                  + HLSG * AMIN1(0.0, VELGJO(I))
            DISPL       = HLSF * AMAX1(0.0, VELFJO(I))
     *                  + HLSG * AMAX1(0.0, VELGJO(I))
*DELETE,VEXPLT.302,VEXPLT.303
*D VEXPLT.312
*D DMKR008.7
*D VEXPLT.314,315
*D DMKR008.8
*D VEXPLT.317
            DISPK       = DISPK + AVOL(K) * ARAT(I) * AVK * DT
     *                  * (FRICFK * AVRF * VELFJO(I) * VELFJO(I)
     *                  +  FRICGK * AVRG * VELGJO(I) * VELGJO(I))
C
            DISPL       = DISPL + AVOL(L) * ARAT(I+1) * AVL * DT
     *                  * (FRICFL * AVRF * VELFJO(I) * VELFJO(I)
     *                  +  FRICGL * AVRG * VELGJO(I) * VELGJO(I))
*/    PUT PV WORK SEMI-IMPLICITLY IN EQFINL
*D HXCR008.6,7
            SOURCE(K)   = SOURCE(K)
     *                  + ((UFJ(I) - UO(KX)) + PO(KX) / RHOFJ(I)) * CONMF
     *                  + ((UGJ(I) - UO(KX)) + PO(KX) / RHOGJ(I)) * CONMG
*D HXCR008.13,14
            SOURCE(L)   = SOURCE(L)
     *                  - ((UFJ(I) - UO(LX)) + PO(LX) / RHOFJ(I)) * CONMF
     *                  - ((UGJ(I) - UO(LX)) + PO(LX) / RHOGJ(I)) * CONMG
*/    PUT PV WORK SEMI-IMPLICITLY IN PRESEQ
*D PRESEQ.101,102
            TLF         = PCMF(L-5) * TMF
     *                  + PCEF(L-5) * (TEF + TMF * PO(LTV) / RHOFJ(I))
```

TABLE A-2. (continued)

```
C
            TLG             = PCMG(L-5) *  TMG
     *                      + PCEG(L-5) * (TEG + TMG *  PO(LTV) / RHOGJ(I))
     *                      + PCMA(L-5) *  TMA
*D PRESEQ.136,137
            TKF             = PCMF(K-5) *  TMF
     *                      + PCEF(K-5) * (TEF + TMF * PO(KTV) / RHOFJ(I))
C
            TKG             = PCMG(K-5) *  TMG
     *                      + PCEG(K-5) * (TEG + TMG * PO(KTV) / RHOGJ(I))
     *                      + PCMA(K-5) *  TMA
*/    DELETE THE EXPLICIT PV WORK FROM VEXPLT
*D VEXPLT.318,320
C        ADD DISSIPATION TERMS TO THE SOURCE TERM
C
*D VEXPLT.323
         SOURCE(KX) = SOURCE(KX) + DISPK
*D VEXPLT.326
         SOURCE(LX) = SOURCE(LX) + DISPL
*/    DELETE THE EXPLICIT PV WORK FROM ACCUM
*D OMKR017.249,256
```

APPENDIX B
QUALITY ASSURANCE PROCEDURE FOR DEVELOPMENT OF THE RELAP5 RESAR-3S SMALL BREAK MODEL

APPENDIX B
QUALITY ASSURANCE PROCEDURE FOR DEVELOPMENT OF THE RELAP5 RESAR-3S SMALL BREAK MODEL

The following is a quality assurance procedure that was developed, and followed, to assure the accuracy of the RELAP5 RESAR-3S small break model.

1. System Nodalization Diagram--Based on FSAR information and knowledge of the transient to be run, a complete system nodalization diagram is constructed. All components and subsystems required for the calculation are included in the nodalization diagram. This process allows a straightforward determination of the type of data/information required to compile a plant data base (Step 2).

2. Plant Data Base--A plant data base is compiled to include all the data/information required to develop the plant model. The contents of the data base are of the form of actual plant drawings, technical specifications, operating manuals, FSARs, etc. (or copies of the same), and are limited to first hand sources (if possible). This step allows checking of all data/information back to an original source, rather than relying on second hand information. The data base also includes a table of contents that uniquely specifies all material contained therein. The table of contents lists all drawings by drawing number and revision number (if any), and all other sources of data/information by title, date, and revision number (if any). The table of contents is sufficiently detailed to allow duplication of the plant data base by an independent party if required.

3. Calculation Worksheets--A set of worksheets, which completely document all the calculations required to develop the input model, is compiled. Data used in a calculation are referenced to a drawing or other source of data listed in the plant data base (Step 2). Each calculation is written out in sufficient detail

to allow easy checking, and any assumption required in the calculation or any "special method" required to derive a given quantity are clearly indicated. If a calculation is a revision of a previous calculation, it is so stated on the worksheet, and the reason for the change is included. Both the initial calculation worksheet and the revised calculation worksheet are kept as part of the worksheet package.

4. Input Deck--The input deck is developed directly from the worksheets compiled in Step 3.

Once the above steps have been completed, the checkout of the system model proceeds as follows:

1. All data used in the calculation worksheets are checked and varified against the references in the plant data base.

2. All calculations are checked for accuracy and completeness.

3. Input deck values are checked against the values developed in the worksheets.

Notification that the calculation worksheets has been checked for accuracy is included on each worksheet by affixing the reviewers name and date (i.e., CHECKED BY _____, DATE _____). The "checked" status on the worksheet means both the calculations and initial data have been checked. Notification that the input deck has been checked for accuracy is included at the start of the input deck, along with the warning that no changes are to be made which would alter the plant model portion of the input, without first providing the appropriate calculation worksheet and input from revisions, and going through the checkout procedure (listed above) for each revision. By following this procedure, the continued accuracy of the input deck is assured.

APPENDIX C
FUEL STORED ENERGY CALCULATION

E. T. Laats

APPENDIX C
FUEL STORED ENERGY CALCULATION

The FRAPCON-2 steady state fuel rod behavior code[a] was used to estimate the initial conditions of the RESAR-3S fuel rods prior to the LOCA events analyzed in this study. First, the hot rod was modeled to operate at constant full power (29.9 kW/m peak power on the hot rod) to determine when during the rod lifetime that maximum centerline temperature and stored energy occurred. That time was found to be 10 days after initial startup, when fuel centerline temperature was about 25 K higher than at beginning of life. Then, the radial temperature profile and stored energy were determined for a typical hot bundle rod, a core average rod, and a rod operating at 90% of core average power.

Presented in this Appendix are a brief description of the FRAPCON-2 code, the input to the FRAPCON-2 code used for this analysis, and the results obtained.

1. FRAPCON-2 DESCRIPTION

The FRAPCON-2 code[1] calculates steady state thermal and mechanical behavior of light water reactor fuel rods under long-term irradiation conditions. FRAPCON-2 is a modular code containing isolated subcodes that model fuel temperatures, considering fuel cracking and relocation; fuel and cladding deformation, including elastic and plastic cladding deformation and creep; and rod internal pressure, including fission gas release effects.

Fuel, cladding, and internal gas properties are modeled by a materials properties subcode, MATPRO-11.[2] FRAPCON-2 also includes the FRAIL-5 subcode that determines the probability of fuel rod failure.

Input to FRAPCON-2 includes axial nodalization and fuel rod design parameters, which are to be supplied by the user. The rod operating

---

a. Idaho National Engineering Laboratory Configuration Control No. H019882B.

history, which specifies the system coolant conditions, axial power distributions, and time dependent rod average power, must also be given.

A detailed description of FRAPCON-2 is available in References C-1 and C-2.

2. FRAPCON-2 INPUT

The FRAPCON-2 input deck for the hot rod (with Westinghouse proprietary information deleted) is listed on Table C-1. The required input to model the rod and coolant channel geometry represent the RESAR-3S 17 x 17 rod and bundle configurations. The FRAPCON-2 model options selected were the PELET deformation model and the FASTGRASS fission gas release model. These selections are based on the recommendations in References C-3 and C-4.

The corewide power distributions used in this study represented values reported in the RESAR-3S Safety Analysis Report. The rod axial power distribution attained a peak-to-average ratio of 1.19 and a corewide radial peak-to-average ratio of 1.41. Thus, the peaking factor at the hot location of the core hot rod was 1.41 x 1.19, or 1.678. For the average rod in the core hot assembly, the radial peak-to-average ratio was assumed to be 1.20, rather than 1.41 as used for the hot rod. The radial power distribution within the fuel pellets was calculated within the FRAPCON-2 code. That power distribution is illustrated in Figure C-1.

To determine the time during operation when maximum stored energy occurred, the power history of the hot rod was divided into two parts. First, the rod was ramped to full power (9.13 kW/ft or 29.9 kW/m at the peak power elevation) at the rate of 3 kW/hr. Then, constant full power operation was maintained for 1000 hrs. It was noted from this calculation that maximum stored energy of the hot rod occurred at 10 days after startup. Then, the three other calculations were performed to represent an average rod in the hot assembly, a core average rod, and a rod operating at 90% of core average power. (These three calculations were needed as input to subsequent thermal-hydraulic calculations.) Each of the three calculations was also subjected to the 3 kW/hr startup ramp and subsequent

TABLE C-1. FRAPCON-2 INPUT DECK.

```
ETLSEA,P2,T77,EC12.
ACCNT,ID=ETL,ORG=2230,CHG=[redacted],BIN=TK9.
RFL,CM=377000,EC=12.
ATTACH,FRPCN2,FRAPX,ID=BNWV1M3.
FRPCN2.
C
RESAR-3S CALCULATION -- HOT ROD
 $FRPCN
  IM =   20,NA =   12,NR =   11,NF =    5,NC =    4,MECHAN =1,NGASR=-2,
 $END
 $FRPCON
  COMP  =      0.,CPL    =0.16457,DCI    =.008357,DCO    = 0.0095,
  DE    =.01177,DEN    =   95.06,DISHSD=[redacted],DP     =.008192,
  DSPG  =[redacted],DSPGW  =[redacted],ENRCH  =      2.6,FGPAV  =[redacted],
  FLUX  =3.9E13,HDISH  =[redacted],HPLT   =0.01346,ICM    =       4,
  IDXGAS=      1,IPLANT=      1,IO     =       0,JDLPR  =       1,
  JN    =     11,JST    =      1,NCPT   =       0,NSP    =       0,
  NUNITS=      0,ROUGHC=[redacted],ROUGHF=[redacted],TOTL   = 3.6585,
  VS    =[redacted],
  CLDWKS=[redacted],CREPHR=     10.,                 GRNSIZ=    10.,
  NPRINT=      1,PPMH2O=      0.,PPMN2 =     15.,RSNTR  =    93.2,
  TSINT =[redacted],
  GO(1) = 3552.,
  TW(1) = 500.,
  P2(1) = 1.535+7,
  QF(1) = 0.27,0.97,1.13,1.19,1.19,1.19,1.18,1.14,1.10,0.91,0.22,
  X(1)  = 0.,0.366,0.732,1.098,1.463,1.829,2.195,2.55,2.93,
          3.29,3.6585,
  OMPY(1)= 0.1,3.0,6.0,9.0,12.0,15.0,16.06,17.84,18.0,21.0,
           21.41,24.0,8*25.16,
  TIME(1)=0.01,0.042,0.063,0.125,0.167,0.208,0.223,0.248,
          0.25,0.292,0.297,0.333,0.349,1.,5.,10.,15.,20.,25.,30.,
 $END
```

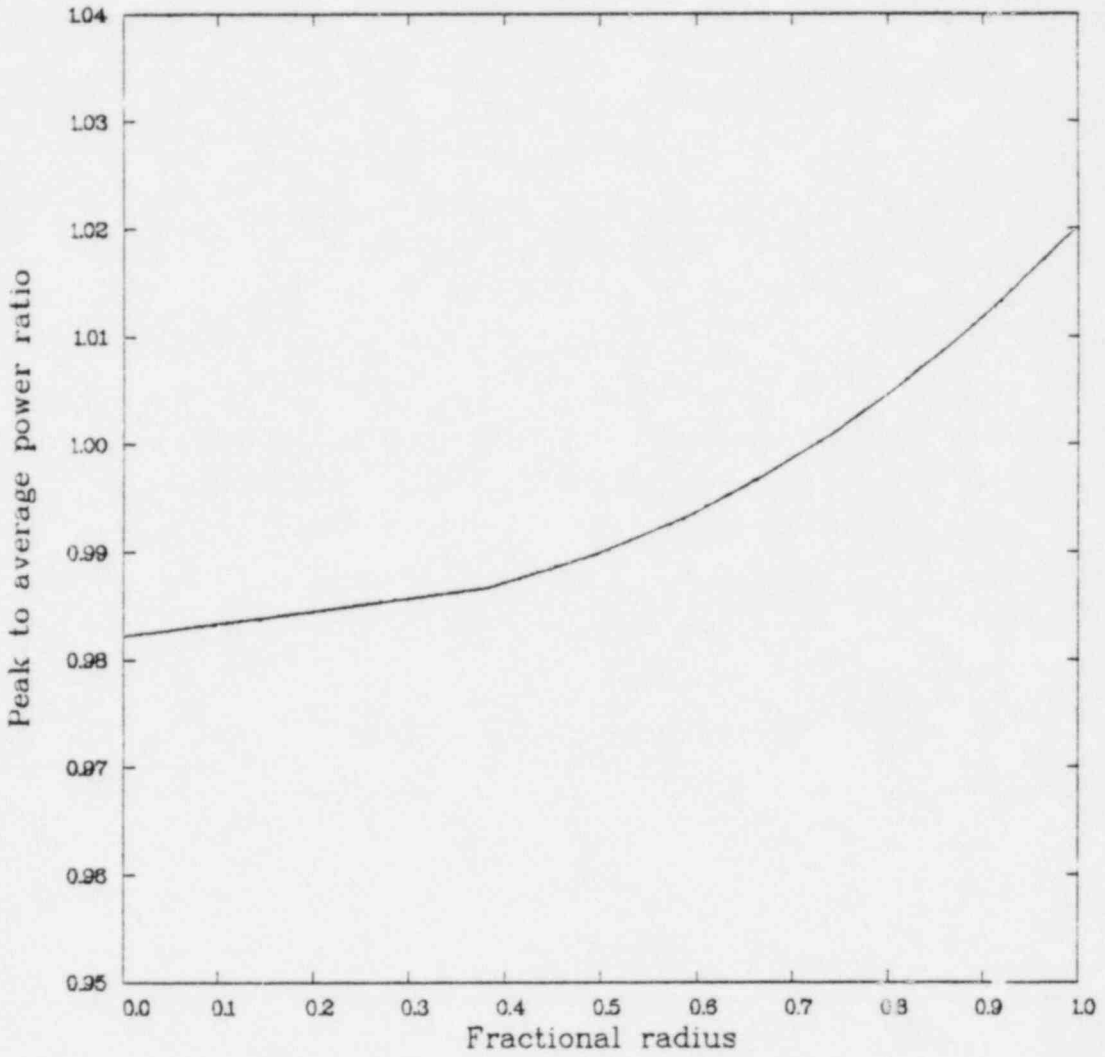

Figure C-1. Radial power distribution in the fuel pellets.

constant power operation to 10 days. The radial temperature distribution noted at the end of the 10 day irradiation, was subsequently used to initialize the thermal-hydraulic calculations.

3. RESULTS

The results of the four FRAPCON-2 calculations (hot rod, hot assembly, core average, 90% of core average) are summarized in Figure C-2. Shown are four curves representing the radial temperature profile for each case, at the rod hot spot. These profiles were obtained at 10 days after startup. The fuel centerline temperature of each curve shown in Figure C-2, is plotted in Figure C-3 against local power.

Since maximum stored energy occurred at 10 days, no significant effects of long term irradiation were noted, such as fission gas release, cladding creepdown, and fuel densification. Thus, the boundary conditions and general state of the fuel rods, as subsequently modeled by the thermal-hydraulic codes, reflect fresh fuel rods. The only exception is decay heat, which was assumed to be 91% of the heat generated if the ANS 73 model was used.

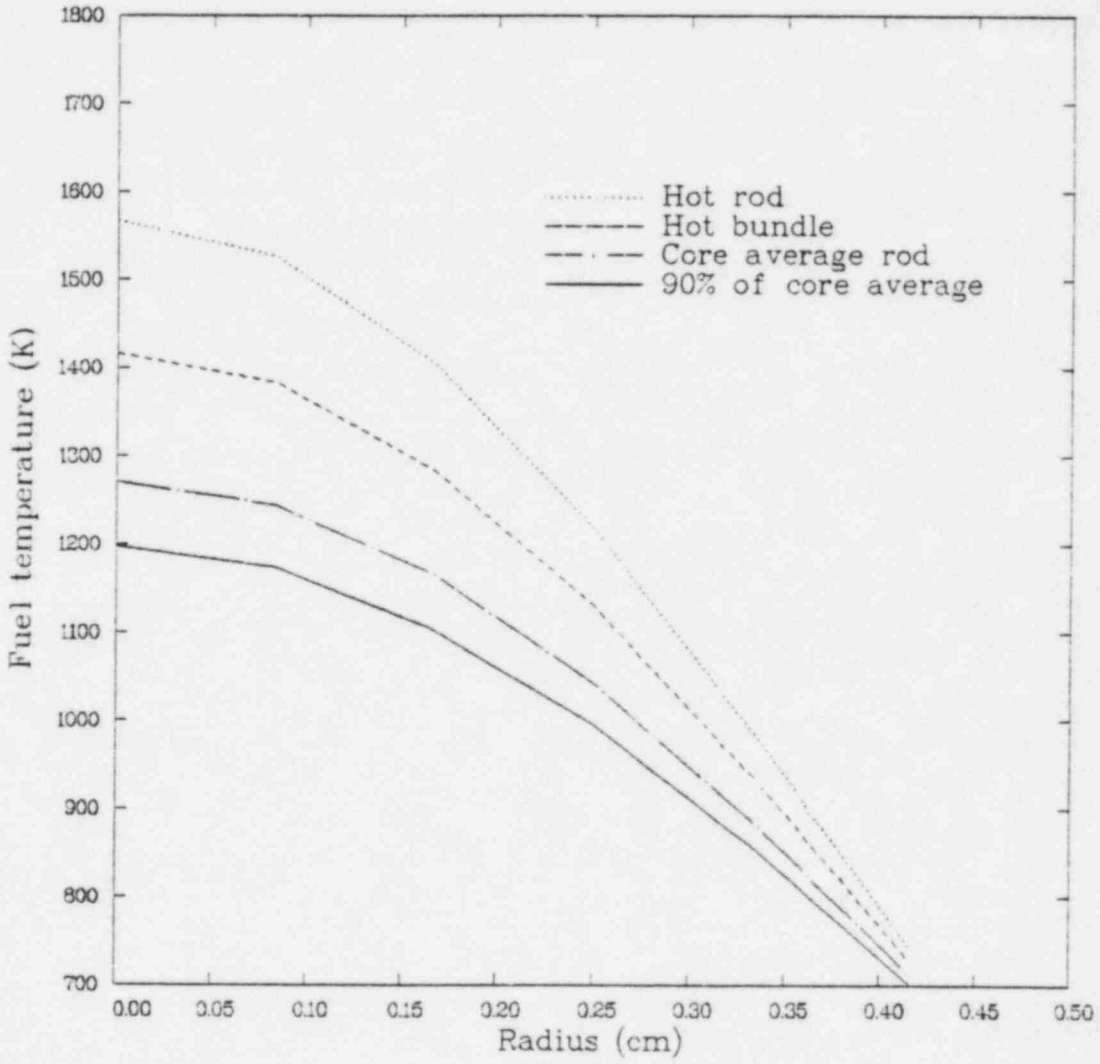

Figure C-2. Radial temperature profiles from FRAPCON-2 calculations.

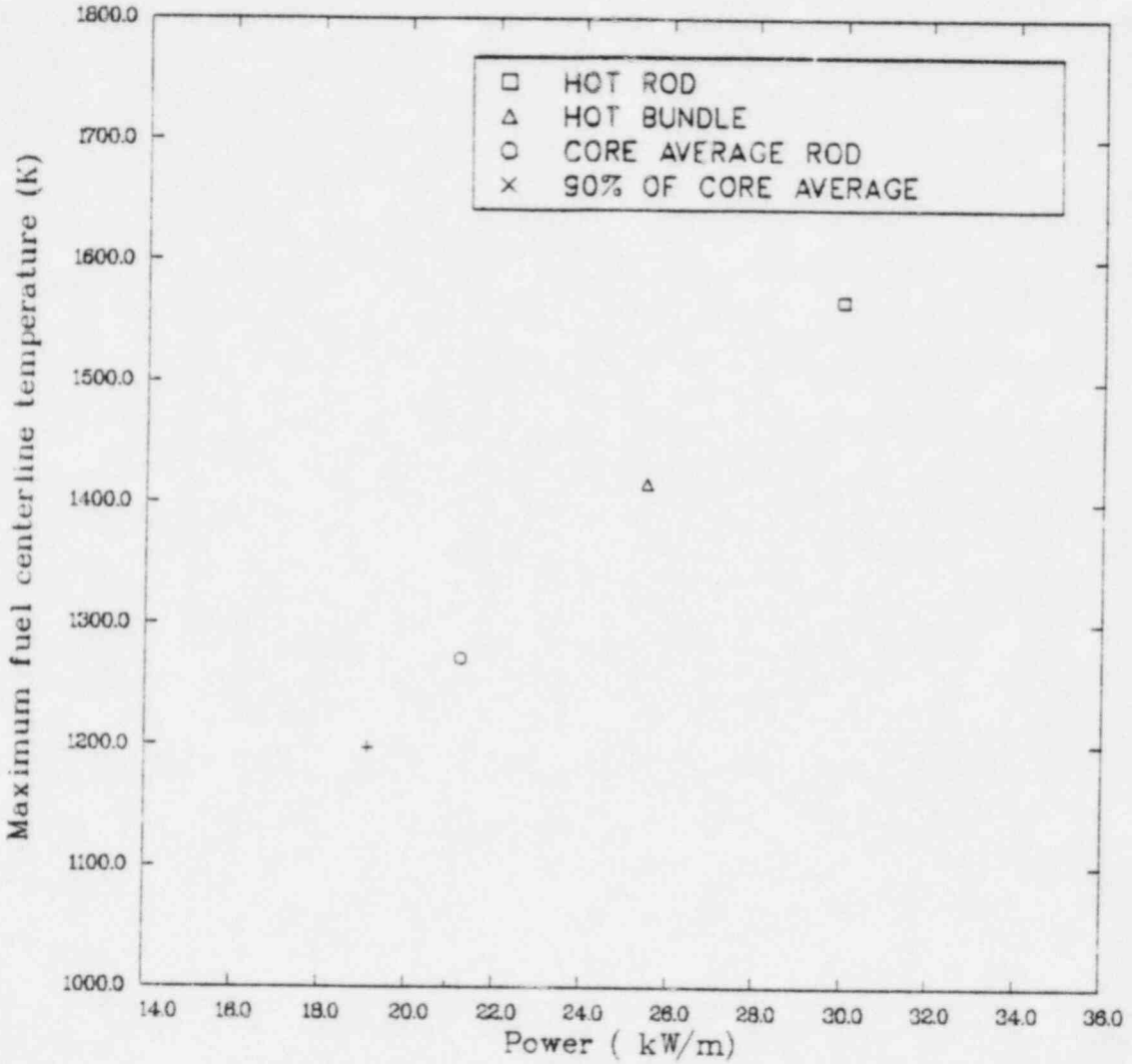

Figure C-3. Fuel centerline temperatures from FRAPCON-2 calculations vs. local power.

REFERENCES

C-1. G. A. Berna et al., FRAPCON-2: A Computer Code for the Calculation of Steady State Thermal-Mechanical Behavior of Oxide Fuel Rods, NUREG/CR-1845, December 1980.

C-2. D. L. Hagrman et al., MATPRO-Version 11 (Revision 1): A Handbook of Materials Properties for Use in the Analysis of Light Water Reactor Fuel Behavior, NUREG/CR-0497, TREE-1280, Rev. 1, February 1980.

C-3. E. T. Laats et al., Independent Assessment of the Steady State Fuel Rod Analysis Code FRAPCON-2, EGG-CAAP-5335, January 1981.

C-4. G. A. Berna et al., FRACPON-2 Development Assessment, NUREG/CR-1949, PNL-3849, July 1981.